

Potent Inhibitors of the Hepatitis C Virus NS3 Protease: Design and Synthesis of Macrocyclic Substrate-Based β -Strand Mimics

Nathalie Goudreau, Christian Brochu, Dale R. Cameron,[†] Jean-Simon Duceppe, Anne-Marie Faucher, Jean-Marie Ferland, Chantal Grand-Maitre, Martin Poirier, Bruno Simoneau, and Youla S. Tsantrizos*

Departments of Chemistry, Boehringer Ingelheim (Canada) Ltd., Research and Development, 2100 Cunard Street, Laval (Quebec), Canada H7S 2G5

ytsantrizos@lav.boehringer-ingelheim.com

Received April 28, 2004

The virally encoded NS3 protease is essential to the life cycle of the hepatitis C virus (HCV), an important human pathogen causing chronic hepatitis, cirrhosis of the liver, and hepatocellular carcinoma. The design and synthesis of 15-membered ring β -strand mimics which are capable of inhibiting the interactions between the HCV NS3 protease enzyme and its polyprotein substrate will be described. The binding interactions between a macrocyclic ligand and the enzyme were explored by NMR and molecular dynamics, and a model of the ligand/enzyme complex was developed.

Introduction

Small molecules which can attenuate the function of a biological process by mimicking the secondary structure of proteins, or the critical molecular recognition elements (structural *hot spots*) between polypeptides and proteins, are of enormous scientific interest.¹ Such interactions play a key role in numerous cellular functions (e.g., protein glycosylation,² intracellular recognition,³ proteolysis, and others) that can be of particular relevance in biological targets associated with important disease areas, including viral infections. However, the key challenge in designing these small molecular mimics is that, unlike the structurally unique peptides found at the contact points between two large biomolecules, short peptides are conformationally heterogeneous and exhibit low affinity for their intended binding sites. Nonetheless, small peptidic ligands can provide valuable research tools in structure-based drug design and important leads in drug discovery efforts that target therapeutically relevant protein–protein or protein–polypeptide interactions.

In our quest for the discovery of a small molecule which could block replication of the hepatitis C virus (HCV), the critical interactions between the virally encoded NS3 serine protease and its polyprotein substrate(s) were investigated. The HCV single-stranded RNA genome encodes a polyprotein of approximately 3000 amino acid residues, which must be proteolytically processed into at least four structural and six nonstructural mature viral proteins. The structural proteins are cleaved from the

polyprotein by host enzymes, whereas the nonstructural (NS) proteins are processed by two virally encoded proteases, the NS2/NS3 and the NS3 proteases.⁴ The NS3 protein is a multifunctional enzyme which harbors protease activity at its *N*-terminal domain and RNA helicase/ATPase activity at its *C*-terminal domain. The NS3 protease domain is responsible for cleavage at four sites along the HCV polyprotein nonstructural region (a >2000 amino acid polyprotein substrate) and is essential for the release of most HCV nonstructural proteins, including the RNA-dependent RNA polymerase enzyme (NS5B). Therefore, the NS3 protease is essential for viral replication in vivo, and consequently, it is an important target for drug discovery efforts.^{4–6}

Some of the recognition elements dictating substrate specificity and the catalytic efficiency of the HCV NS3 serine protease were initially probed using a number of synthetic dodecamer substrates and hexapeptide ligands which resembled the *N*-terminal proteolysis products formed upon cleavage of the natural HCV polyprotein.^{7,8} Hexapeptide ligands, such as compound **1**, were found to be competitive inhibitors of the enzyme and provided the first lead structures for the design of peptidomimetic inhibitors of the HCV NS3 protease.^{9–11} In addition, such peptides served as tools in further exploring the interactions between substrate-based ligands and the NS3

* To whom correspondence should be addressed.

[†] Present address: Micrologix Biotech, Inc., BC Research Complex, 3650 Westbrook Mall, Vancouver BC V6S 2L2, Canada.

(1) (a) Cochran, A. G. *Curr. Opin. Chem. Biol.* **2001**, *5*, 654. (b) Peczu, M. W.; Hamilton, A. D. *Chem. Rev.* **2000**, *100*, 2479. (c) Cochran, A. G. *Chem. Biol.* **2000**, *7*, R85.

(2) Weerapana E.; Imperiali, B. *Org. Biomol. Chem.* **2003**, *1*, 93.

(3) Loregian, A.; Marsden, H. S.; Palù, G. *Rev. Med. Virol.* **2002**, *12*, 239.

(4) (a) De Francesco, R.; Tomei, L.; Altamura, S.; Summa, V.; Migliaccio, G. *Antiviral Res.* **2003**, *58*, 1. (b) Tan, S.-L.; Pause, A.; Shi, Y.; Sonenberg, N. *Nature Rev. Drug Discovery* **2002**, *1*, 867. (c) Reed, K. E.; Rice, C. M. *Curr. Top. Microbiol. Immunol.* **2000**, *242*, 55.

(5) Kolykhalov, A. A.; Mihalik, K.; Feinstone, S. M.; Rice, C. M. *J. Virol.* **2000**, *74*, 2046.

(6) Foy, E.; Li, K.; Wang, C.; Sumpter, R., Jr.; Ikeda, M.; Lemon, S. M.; Gale, M., Jr. *Science* **2003**, *300*, 1145.

(7) Llinàs-Brunet, M.; Bailey, M.; Fazal, G.; Goulet, S.; Halmos, T.; LaPlante, S.; Maurice, R.; Poirier, M.; Poupart, M.-A.; Thibeault, D.; Wernic, D.; Lamarre, D. *Bioorg. Med. Chem. Lett.* **1998**, *8*, 1713.

(8) Steinkühler, C.; Biasiol, G.; Brunetti, M.; Urbani, A.; Koch, U.; Cortese, R.; Pessi, A.; De Francesco, R. *Biochemistry* **1998**, *37*, 8899.

protease by NMR,^{12–15} molecular modeling, and crystallography.¹⁶ However, the inherent conformational flexibility of linear peptides, in addition to the solvent-exposed and shallow nature of the NS3 protease active site, made optimization of these structures into a *druglike* compound an extremely challenging endeavor.

Recently, we reported on the design and synthesis of macrocyclic inhibitors of the NS3 protease which are orally absorbed and inhibit replication of HCV RNA in a cell-based replicon assay.¹⁷ We demonstrated that these compounds possess many of the desirable properties of a druglike archetype, thus bridging the gap between the inhibitors of HCV NS3 protease that have been reported so far,^{7,9–11,16,18} and a clinically useful antiviral agent for

the treatment of hepatitis C in humans.^{17,19} In this paper, the design and synthesis of the initial 15-membered ring peptidomimetic scaffold, which led to the discovery of the clinical antiviral agent BILN 2061 (**2**),¹⁹ will be discussed. Some of the critical structural studies which guided the design of the β -strand scaffold, mimicking the NS3-bound conformation of the *N*-terminal cleavage products of the HCV polyprotein substrate(s), will be presented. The synthesis and preliminary evaluation of the structure–activity relationship (SAR) of these inhibitors will also be described. The results of this investigation illustrate that even in the absence of an enzyme–ligand cocrystal structure, it is possible to obtain valuable structural data that can successfully guide a rational drug design program.²⁰

(9) Llinàs-Brunet, M.; Bailey, M.; Déziel, R.; Fazal, G.; Gorys, V.; Goulet, S.; Halmos, T.; Maurice, R.; Poirier, M.; Poupart, M.-A.; Rancourt, J.; Thibeault, D.; Wernic, D.; Lamarre, D. *Bioorg. Med. Chem. Lett.* **1998**, *8*, 2719.

(10) P. Ingallinella, P.; Altamura, S.; Bianchi, E.; Taliani, M.; Ingenito, R.; Cortese, R.; De Francesco, R.; Steinkühler, C.; Pessi, A. *Biochemistry* **1998**, *37*, 8906.

(11) Llinàs-Brunet, M.; Bailey, M.; Fazal, G.; Ghio, E.; Gorys, V.; Goulet, S.; Halmos, T.; Maurice, R.; Poirier, M.; Poupart, M.-A.; Rancourt, J.; Thibeault, D.; Wernic, D.; Lamarre, D. *Bioorg. Med. Chem. Lett.* **2000**, *10*, 2267.

(12) LaPlante, S. R.; Cameron, D. R.; Aubry, N.; Lefebvre, S.; Kukolj, G.; Maurice, R.; Thibeault, D.; Lamarre, D.; Llinàs-Brunet, M. *J. Biol. Chem.* **1999**, *274*, 18618.

(13) Cicero, D. O.; Barbato, G.; Koch, U.; Ingallinella, P.; Bianchi, E.; Nardi, M. C.; Steinkühler, C.; Cortese, R.; Matassa, V.; De Francesco, R.; Pessi, A.; Bazzo, R. *J. Mol. Biol.* **1999**, *289*, 385.

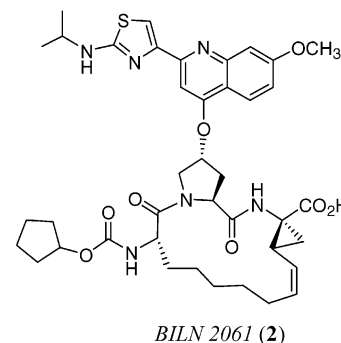
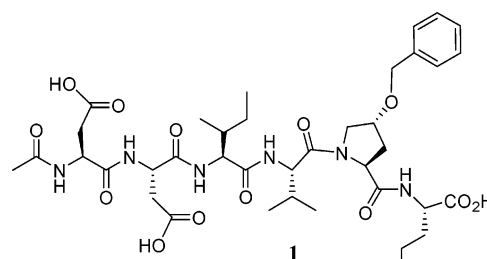
(14) Barbato, G.; Cicero, D. O.; Cordier, F.; Narjes, F.; Gerlach, B.; Sambucini, S.; Grzesiek, S.; Matassa, V. G.; De Francesco, R.; Bazzo, R. *EMBO J.* **2000**, *19*, 1195.

(15) LaPlante, S. R.; Aubry, N.; Bonneau, P. R.; Kukolj, G.; Lamarre, D.; Lefebvre, S.; Li, H.; Llinàs-Brunet, M.; Plouffe, C.; Cameron, D. R. *Bioorg. Med. Chem. Lett.* **2000**, *10*, 2271.

(16) Di Marco, S.; Rizzi, M.; Volpari, C.; Walsh, M. A.; Narjes, F.; Colarusso, S.; De Francesco, R.; Matassa, V. G.; Sollazzo, M. *J. Biol. Chem.* **2000**, *275*, 7152.

(17) (a) Tsantrizos, Y. S.; Bolger, G.; Bonneau, P.; Cameron, D. R.; Goudreau, N.; Kukolj, G.; LaPlante, S. R.; Llinàs-Brunet, M.; Nar, H.; Lamarre, D. *Angew. Chem., Int. Ed.* **2003**, *42*, 1356. (b) Tsantrizos, Y. S.; Cameron, D. R.; Faucher, A.-M.; Ghio, E.; Goudreau, N.; Halmos, T.; Llinàs-Brunet, M. PTC International Application [Boehringer Ingelheim (Canada) Ltd.] WO 00/59929; October 2000.

(18) (a) Perni, R. B.; Pitlik, J.; Britt, S. D.; Court, J. J.; Courtney, L. F.; Deininger, D. D.; Farmer, L. J.; Gates, C. A.; Harbeson, S. L.; Levin, R. B.; Lin, C.; Lin, K.; Moon, Y.-C.; Luong, Y.-P.; O'Malley, E. T.; Rao, B. G.; Thomson, J. A.; Tung, R. D.; Van Drie, J. H.; Wei, Y. *Bioorg. Med. Chem. Lett.* **2004**, *14*, 1441. (b) Lamar, J.; Victor, F.; Snyder, N.; Johnson, R. B.; Wang, Q. M.; Glass, J. I.; Chen, S.-H. *Bioorg. Med. Chem. Lett.* **2004**, *14*, 263. (c) Victor, F.; Lamar, J.; Snyder, N.; Yip, Y.; Guo, D.; Yumibe, N.; Johnson, R. B.; Wang, Q. M.; Glass, J. I.; Chen, S.-H. *Bioorg. Med. Chem. Lett.* **2004**, *14*, 257. (d) Yip, Y.; Victor, F.; Lamar, J.; Johnson, R.; Wang, Q. M.; Barket, D.; Glass, J.; Jin, L.; Liu, L.; Venable, D.; Wakulchik, M.; Xie, C.; Heinz, B.; Villarreal, E.; Colacino, J.; Yumibe, N.; Tebbe, M.; Munroe, J.; Chen, S.-H. *Bioorg. Med. Chem. Lett.* **2004**, *14*, 251. (e) Johansson, A.; Poliakov, A.; Akerblom, E.; Wiklund, K.; Lindeberg, G.; Winiwarter, S.; Danielson, U. H.; Samuelsson, B.; Hallberg, A. *Bioorg. Med. Chem.* **2003**, *11*, 2551. (f) Hegde, V. R.; Pu, H.; Patel, M.; Das, P. R.; Butkiewicz, N.; Arreaza, G.; Gullo, V. P.; Chan, T.-M. *Bioorg. Med. Chem. Lett.* **2003**, *13*, 2925. (g) Orvieto, F.; Koch, U.; Matassa, V. G.; Muraglia, E. *Bioorg. Med. Chem. Lett.* **2003**, *13*, 2745. (h) Colarusso, S.; Koch, U.; Gerlach, B.; Steinkühler, C.; De Francesco, R.; Altamura, S.; Matassa, V. G.; Narjes, F. *J. Med. Chem.* **2003**, *46*, 345. (i) Orvieto, F.; Koch, U.; Matassa, V. G.; Muraglia, E. *Bioorg. Med. Chem. Lett.* **2003**, *13*, 2745. (j) Andrews, D. M.; Chaignot, H.; Coomber, B. A.; Good, A. C.; Hind, S. L.; Johnson, M. R.; Jones, P. S.; Mills, G.; Robinson, J. E.; Skarzynski, T.; Slater, M. J.; Somers, D. O'N. *Org. Lett.* **2002**, *4*, 4479. (k) Narjes, F.; Koehler, K. F.; Koch, U.; Gerlach, B.; Colarusso, S.; Steinkühler, C.; Brunetti, M.; Altamura, S.; De Francesco, R.; Matassa, V. G. *Bioorg. Med. Chem. Lett.* **2002**, *12*, 701. (l) Colarusso, S.; Gerlach, B.; Koch, U.; Muraglia, E.; Conte, I.; Stansfield, I.; Matassa, V. G.; Narjes, F. *Bioorg. Med. Chem. Lett.* **2002**, *12*, 705. (m) Han, W.; Hu, Z.; Jiang X.; Decicco, C. P. *Bioorg. Med. Chem. Lett.* **2000**, *10*, 711. (n) Dunsdon, R. M.; Greening, J. R.; Jones, P. S.; Jordan, S.; Wilson, F. X. *Bioorg. Med. Chem. Lett.* **2000**, *10*, 1577. (o) Marchetti, A.; Ontoria, J. M.; Matassa, V. G. *Synlett* **1999**, *SI*, 1000.



Results and Discussion

Design of Substrate-Based, β -Strand Mimics as Potent Inhibitors of the HCV NS3 Protease. During the past decade, considerable effort has been devoted to the design and synthesis of small molecules which can mimic the α -helical,²¹ β -turn,²² or β -strand²³ secondary structures of proteins. Many of the scaffolds that have been designed are undoubtedly inspired by nature's nonribosomally formed secondary metabolites which are

(19) (a) Llinàs-Brunet, M.; Bailey, M. D.; Bolger, G.; Brochu, C.; Faucher, A.-M.; Ferland, J. M.; Garneau, M.; Ghio, E.; Gorys, V.; Grand-Maitre, C.; Halmos, T.; Lapeyre-Paquette, N.; Liard, F.; Poirier, M.; Rhéaume, M.; Tsantrizos, Y. S.; Lamarre, D. *J. Med. Chem.* **2004**, *47*, 1605. (b) Lamarre, D.; Anderson, P. C.; Bailey, M.; Beaulieu, P.; Bolger, G.; Bonneau, P.; Bös, M.; Cameron, D.; Cartier, M.; Cordingley, M. G.; Faucher, A.-M.; Goudreau, N.; Kawai, S. H.; Kukolj, G.; Lagacé, L.; LaPlante, S. R.; Narjes, H.; Poupart, M.-A.; Rancourt, J.; Sentjens, R. E.; St George, R.; Simoneau, B.; Steinmann, G.; Thibeault, D.; Tsantrizos, Y. S.; Weldon, S. M.; Yong, C.-L.; Llinàs-Brunet, M. *Nature* **2003**, *426*, 186. (c) Rice, C. M. *Nature* **2003**, *426*, 129.

(20) Davis, A. M.; Teague, S. J.; Kleywegt, G. *J. Angew. Chem., Int. Ed.* **2003**, *42*, 2718.

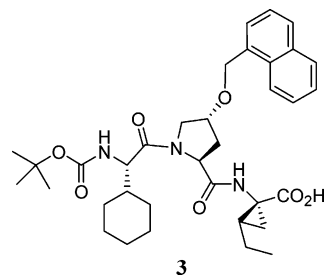
(21) (a) Kutzki, O.; Park, H. S.; Ernst, J. T.; Orner B. P.; Yin, H.; Hamilton, A. D. *J. Am. Chem. Soc.* **2002**, *124*, 11838. (b) Banerjee, R.; Basu, G.; Chène, P.; Roy, S. *J. Peptide Res.* **2002**, *60*, 88.

(22) (a) Lucke, A. J.; Tyndall, J. D. A.; Singh, Y.; Fairlie, D. P. *J. Mol. Graph. Mod.* **2003**, *21*, 341. (b) Hanessian, S.; McNaughton-Smith, G.; Lombart, H.-G.; Lubell, W. D. *Tetrahedron* **1997**, *53*, 12789.

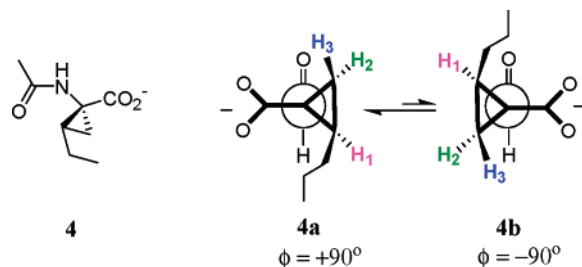
often composed of unusual amino acid fragments and are constrained into cyclic peptides with unique bioactive conformations. Introduction of nature's preorganization elements to synthetic scaffolds has provided a wealth of peptidomimetic compounds with diverse structural, physical, and conformational properties that have been exploited in supramolecular and combinatorial chemistry²⁴ as well as chemical biology and medicinal chemistry.^{1,25} On the basis of this knowledge, macrocyclic peptides which adopt an extended β -strand conformation have also been explored as substrate mimics of metallo, aspartic, cysteine, and serine proteases;^{23,25} the HCV NS3 protease is an example of the latter class of enzymes. However, the HCV NS3 enzyme is fairly unique among serine proteases in that it is activated by its structure-modifying cofactor NS4A (a 54-residue peptide).²⁶ The interactions between the NS4A cofactor and the NS3 protease are known to induce conformational changes that significantly reduce (but not entirely eliminate) the plasticity of the enzyme, thus enhancing its catalytic power. Induced-fit conformational changes of the enzyme upon binding of a product-based ligand have also been reported.²⁷

In the course of our initial investigations, NMR studies of the NS3-bound hexapeptide **1** revealed that this ligand binds in an extended, β -strand conformation and its interactions with the enzyme involve predominately the P1–P3 residues.^{12,28–30} Additional NMR studies with an analogue of tripeptide **3**, having a more optimized 1-amino-

nocyclopropylcarboxylic acid (ACCA) moiety at P1,^{11,37a} confirmed that the backbone of shorter peptides also adopts the extended β -strand conformation upon binding to the NS3.¹⁵ In addition, the structural differences between the free (in solution) and the NS3-bound state of ligand **3** were explored by both NMR and computational studies.



The conformation of the NS3-bound tripeptide **3** was found to be distinctly different from that of its free state. Conformational analysis of an ionized and solvated model compound of the P1 residue, such as compound **4**, by semiempirical quantum mechanics calculations identified two low energy conformations for the P1 ethyl ACCA moiety, **4a** and **4b** (ϕ of approximately $+90^\circ$ and -90° , respectively), and calculated an energy difference of ~ 1.1 kcal/mol in favor of **4a** (with an estimated ratio of $\sim 4:1$). The ROESY NMR spectrum of ligand **3** (Figure 1a) confirmed that in the free state the predominant conformation of its P1 moiety corresponded to that of **4a**, in agreement with the computational studies. A strong NOE cross-peak between the P1 amide NH and its H_1 proton and a weaker NOE between the NH and the H_2 (*pro-R*) proton were clearly observed, whereas NOE interaction between the NH and the H_3 (*pro-S*) proton could not be detected. The combined NOE data was consistent with a preferred ϕ angle of approximately $+90^\circ$ for the P1 residue of the free ligand **3**, as shown in Figure 1a.



In contrast, transferred NOESY (TRNOESY)³¹ NMR experiments using compound **3** in the presence of the

(23) (a) Bartlett, P. A.; Rezac, M.; Olson, S.; Phillips, S. PTC International Application (The Regents of the University of California) WO 02/099045; December 2002. (b) Dumez, E.; Snaith, J. S.; Jackson, R. F. W.; McElroy, A. B.; Overington, J.; Wythes, M. J.; Withka, J. M.; McLellan, T. J. *J. Org. Chem.* **2002**, *67*, 4882. (c) Reid, R. C.; Kelso, M. J.; Scanlon, M. J.; Fairlie, D. P. *J. Am. Chem. Soc.* **2002**, *124*, 5673. (d) Glenn, M. P.; Pattenden, L. K.; Reid, R. C.; Tyssen, D. P.; Tyndall, J. D. A.; Birch, C. J.; Fairlie, D. P. *J. Med. Chem.* **2002**, *45*, 371. (e) Nowick, J. S.; Smith, E. M.; Ziller, J. W.; Shaka, A. J. *Tetrahedron* **2002**, *58*, 727. (f) Ripka, A. S.; Satyshur, K. A.; Bohacek, R. S.; Rich, D. H. *Org. Lett.* **2001**, *3*, 2309. (g) Mak, C. C.; Le, V.-D.; Lin, Y.-C.; Elder, J. H.; Wong, C.-H. *Bioorg. Med. Chem. Lett.* **2001**, *11*, 219. (h) Tyndall, J. D. A.; Fairlie, D. P. *Curr. Med. Chem.* **2001**, *8*, 893. (i) Tian, Z.-Q.; Brown, B. B.; Mack, D. P.; Hutton, C. A.; Bartlett, P. A. *J. Org. Chem.* **1997**, *62*, 514. (j) Nowick, J. S.; Pairish, M.; Lee, I. Q.; Holmes, D. L.; Ziller, J. W. *J. Am. Chem. Soc.* **1997**, *119*, 5413. (k) Boumendjel, A.; Roberts, J. C.; Hu, E.; Pallai, P. V. *J. Org. Chem.* **1996**, *61*, 4434. (l) Smith, A. B.; Hirschmann, R.; Pasternak, A.; Guzman, M. C.; Yokoyama, A.; Sprengeler, P. A.; Darke, P. L.; Emini, E. A.; Schleif, W. A. *J. Am. Chem. Soc.* **1995**, *117*, 11113. (m) Martin, S. F.; Oalman, C. J.; Linas, S. *Tetrahedron* **1993**, *49*, 3532.

(24) (a) Glenn, M. P.; Kelso, M. J.; Tyndall, J. D. A.; Fairlie, D. P. *J. Am. Chem. Soc.* **2003**, *125*, 640. (b) Park, C.; Burgess, K. *J. Comb. Chem.* **2001**, *3*, 257. (c) Singh, Y.; Sokolenko, N.; Kelso, M. J.; Gahan, L. R.; Abbenante, G.; Fairlie, D. P. *J. Am. Chem. Soc.* **2001**, *123*, 333. (d) MacDonald, M.; Aubé, J. *Curr. Org. Chem.* **2001**, *5*, 417. (e) Wipf, P.; Miller, C. P.; Grant, C. M. *Tetrahedron* **2000**, *56*, 9143. (f) Mink, D.; Mecozzi, S.; Rebek, J. *Tetrahedron Lett.* **1998**, *39*, 5709.

(25) (a) Reid, R. C.; Pattenden, L. K.; Tyndall, J. D. A.; Martin, J. L.; Walsh, T.; Fairlie, D. P. *J. Med. Chem.* **2004**, *47*, 1641. (b) Fairlie, D. P.; West, M. L.; Wong, A. K. *Curr. Med. Chem.* **1998**, *5*, 29. (c) Fairlie, D. P.; Abbenante, G.; March, D. R. *Curr. Med. Chem.* **1995**, *2*, 654.

(26) Bartenschlager, R. *J. Viral Hepat.* **1999**, *6*, 165.

(27) Bianchi, E.; Orrù, S.; Piaz, F. D.; Ingenito, R.; Casbarra, A.; Biasiol, G. Koch, U.; Pucci, P.; Pessi, A. *Biochemistry* **1999**, *38*, 13844.

(28) Protease subsite nomenclature: Schechter, I.; Berger, A. *Biochem. Biophys. Res. Commun.* **1967**, *27*, 157.

(29) LaPlante, S. R.; Aubry, N.; Déziel, R.; Ni, F.; Xu, P. *J. Am. Chem. Soc.* **2000**, *122*, 12530.

(30) The role of the P5 and P6 residues was also examined by the IRBM/Merck group using pre-steady-state kinetics. Based on their data, they proposed that the electrostatic surface potential of these residues enhances the collision rates between the peptidic ligand and the active site of NS3 protease; U. Koch, U.; Biasiol, G.; Brunetti, M.; Fattori, D.; Pallaoro, M.; Steinkühler, C. *Biochemistry* **2001**, *40*, 631.

(31) Review: Ni, F. *Prog. Nucl. Magn. Reson. Spectrosc.* **1994**, *26*, 517.

(32) Yao, N.; Reiche, P.; Taremi, S. S.; Prosise, W. W.; Weber, P. C. *Structure* **1999**, *7*, 1353.

(33) Tong, L.; Wengler, G.; Rossmann, M. G. *J. Mol. Biol.* **1993**, *230*, 228.

(34) James, M. N. G.; Sielecki, A. R.; Brayer, G. D.; Delbaere, L. T. J. *J. Mol. Biol.* **1980**, *144*, 43.

(35) Khan, A. R.; Parrish, J. C.; Fraser, M. E.; Smith, W. W.; Bartlett, P. A.; James, M. N. G. *Biochemistry* **1998**, *37*, 16839.

(36) (a) Burgess, K.; Ke, C.-Y. *Synthesis* **1996**, 1463. (b) Burgess, K.; Li, W. *Tetrahedron Lett.* **1995**, *36*, 2725. (c) Burgess, K.; Ho, K.-K. *J. Org. Chem.* **1992**, *57*, 5931.

(37) (a) Rancourt, J.; Cameron, D. R.; Gorys, V.; Lamarre, D.; Poirier, M.; Thibeault, D.; Llinàs-Brunet, M. *J. Med. Chem.* **2004**, *47*, 2511. (b) Bailey, M. D. United States Patent [Boehringer Ingelheim (Canada) Ltd.] US 6,268,207 B1; July 31, 2001.

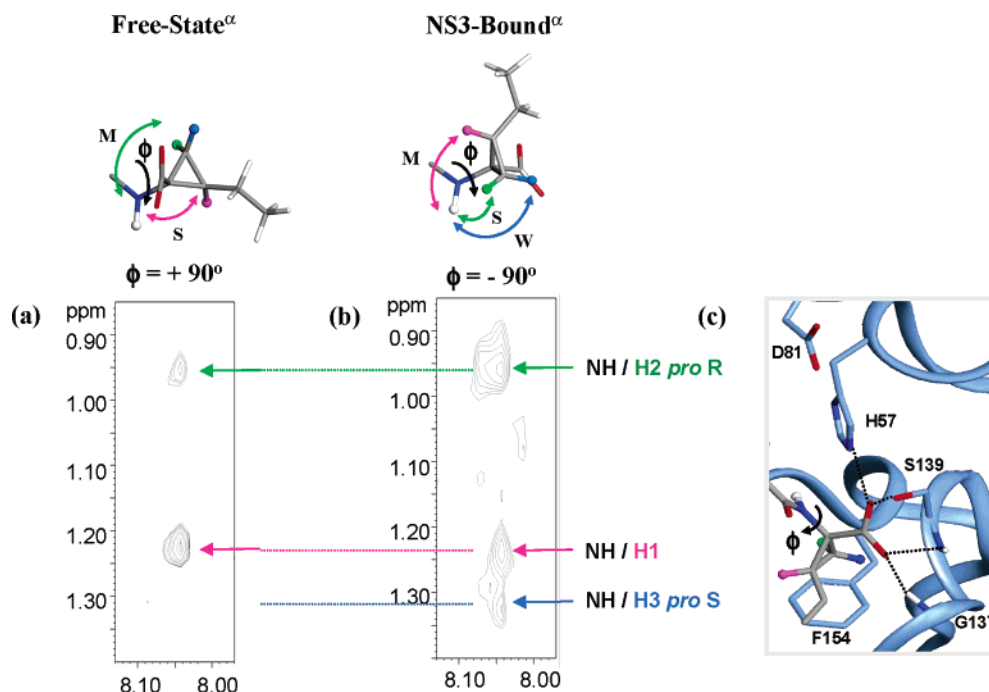


FIGURE 1. Selected region of the NMR spectra of tripeptide **3** (P1 moiety): (a) ROESY NMR spectrum of **3** alone in aqueous buffer; (b) transferred NOESY NMR spectrum of **3** in the presence of the HCV NS3 protease domain (the relative intensities of NOE interactions are indicated as S (strong), M (medium), and W (weak)); (c) model of the P1 moiety of tripeptide **3** docked in the active site of the apo form of NS3 protease. ^aModel compound **4**: colors indicate H₁ (purple), H₂ (green), H₃ (blue).

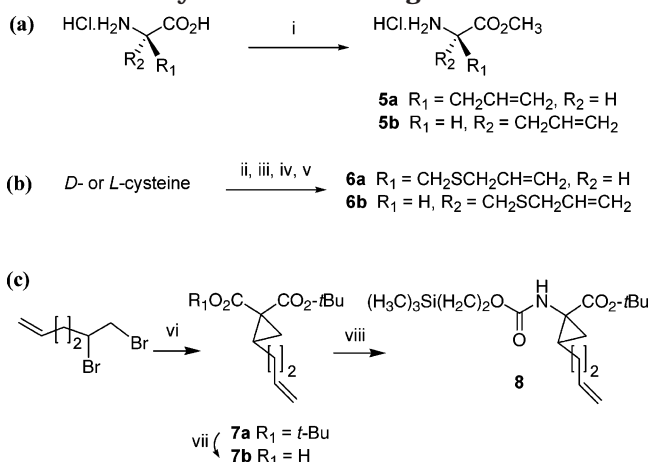
NS3 protease domain provided unambiguous assignment of the bound conformation of the ethyl ACCA moiety (Figure 1b). NOE interactions were observed between the amide NH and all three β -protons (Figure 1b); strong NOE with H₂ (*pro-R*) and weaker NOEs with H₁ and H₃ (*pro-S*). The relative intensities of these NOEs suggested a bound conformation for the P1 moiety with a ϕ angle of approximately -90° (Figure 1b). Docking of the NMR-derived NS3-bound conformation of **3** into the active site of the protease was subsequently attempted, using as guidance the previously published crystal structures of the apo HCV NS3 protease³² and the serine proteases of the *Sindbis* virus³³ and *Streptomyces griseus*.³⁴ This higher energy conformer of **3** (analogous to **4b**, Figure 1b) was consistent with the expected NS3-bound structure (based on the literature),^{31–33} allowing the carboxylate anion of P1 to interact with the oxyanion hole of the active site and possibly the side chains of the catalytic residues H57 and S139 (Figure 1c). Consequently, we concluded that the NH–C $_{\alpha}$ bond of the free ligand **3** had to undergo a rotation of approximately 180° in order to adopt its NS3-bound conformation (Figure 1a vs 1b). The entropic penalty associated with this *realignment* of the ligand would be expected to have a negative impact on its binding energy.

Therefore, we embarked on the design and synthesis of a rigid scaffold which could restrain the P1 ϕ angle to the higher energy conformation (i.e., **4b**, Figure 1b) and simultaneously preorganize the P1–P3 amide backbone exclusively to the *all-trans* geometry (β -strand);¹⁷ the latter is a significant problem with proline-containing linear peptides which exist as mixtures of *cis* and *trans* rotamers. We predicted that covalent linking of the P1 to the P3 side chain, creating a 14- to 16-membered ring structure, could result in a scaffold which in the *free state*

would adopt the desired β -strand NS3-bound conformation. This rigid macrocyclic ligand was expected to pay a lower entropic penalty for binding to the protease and consequently, have a higher affinity for the enzyme than its corresponding acyclic precursor.^{17,35} Furthermore, our NMR data of linear peptides indicated that in the NS3-bound conformation the P3 side chain is mostly solvent-exposed.^{12,15} In contrast, the hydrophobic linker moiety of the macrocyclic scaffold was expected to be properly aligned into the S1–S3 binding pocket so as to favorably interact with the protease. Thus, we predicted that the combined effects of a properly pre-organized rigid scaffold, which closely mimics the enzyme-bound conformation, and a hydrophobic chain that can participate in additional interactions with the active site, would lead to a novel class of very potent peptidomimetic inhibitors of the HCV NS3 protease.

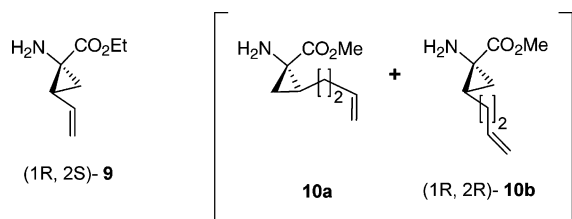
Synthesis of Building Blocks and Inhibitors. To evaluate the biological and conformational properties of β -strand mimics, a variety of P1, P2, and P3 building blocks were synthesized (Schemes 1–3). The allylglycine methyl esters **5a** and **5b** were prepared by treating the corresponding amino acids with anhydrous methanol in the presence of thionyl chloride (Scheme 1a). The cysteine derivatives **6a** and **6b** were prepared by first reacting the corresponding thiols with allyl bromide in the presence of base, followed by protecting the amines as the *tert*-butyl carbamates and then treating with diazomethane. After removal of the Boc protecting group under standard acidic conditions, the acyclic P1 fragments **5a,b** and **6a,b** were used directly in coupling reactions with one of the P2 building blocks.

Both the vinyl (**9**) and homoallyl ACCA (**10**) fragments were synthesized using a slightly modified procedure from that originally reported by Burgess and co-workers

SCHEME 1. Synthesis of P1 Fragments^a

^a Reagents and conditions: (a) synthesis of allylglycine methyl ester P1 analogues (**5a**, **5b**) (i) MeOH/SOCl₂; (b) synthesis of cysteine analogues (**6a** and **6b**) (ii) allyl bromide, NH₄OH, (iii) Boc₂O, K₂CO₃, (iv) CH₂N₂, (v) 4N HCl in dioxane; (c) synthesis of the (1*R*,2*R*)/(1*S*,2*S*)-1-amino-2-homoallylcyclopropyl derivative **8** (vi) BnNEt₃Cl, 50% NaOH_{aq}, di-*tert*-butyl malonate, 23 °C (38%), (vii) *t*-BuOK, H₂O, Et₂O, 0–23 °C (85%), (viii) (PhO)₂P(O)N₃, Et₃N, C₆H₆, reflux, then (CH₃)₃Si(CH₂)₂OH, C₆H₆, reflux (88%).

for the preparation of 2,3-methanomethionine.³⁶ Preparation of the vinyl ACCA moiety (1*R*,2*S*)-**9** was achieved in high enantiomeric purity (>98% ee) as recently reported.³⁷ On the basis of a similar approach (Scheme 1c), the synthesis of the racemic homoallyl ACCA fragment **10** was initiated by the dialkylation of di-*tert*-butylmalonate with 1,2-dibromo-5-hexene,³⁸ followed by selective hydrolysis of the less hindered ester,³⁹ to give the monoester intermediate **7b**. The racemic mixture of **8** (having the allyl side chain *syn* to the *tert*-butyl ester) was subsequently prepared via Curtius rearrangement which was followed by trapping the products as the 2-(trimethylsilyl)ethyl carbamate derivatives.⁴⁰ Compound **8** was used directly in the synthesis of diastereomeric P1–P2 fragments (Scheme 4), which were easily separated by flash column chromatography; the absolute configuration of the (1*R*, 2*R*)-**10b** building block was eventually confirmed.⁴¹



The P2 fragments **15d–f** were prepared from the commercially available Boc-protected *cis*-hydroxyproline methyl ester and each of the three 4-hydroxyquinoline analogues via a Mitsunobu reaction,⁴² followed by saponification of the methyl esters under basic conditions (Scheme 2). Compounds **15a** and **15b** were prepared from the commercially available quinolines **13a** and **13b**,

whereas preparation of **15c** required the synthesis of the precursor 4-hydroxy-7-methoxy-2-phenylquinoline fragment (**13c**).⁴³ Preparation of quinoline **13c** was previously reported as a mixture with its 5-methoxy isomer **14** (3:2 ratio).^{43b} Using a modified protocol,^{43a} we observed that the reaction of *m*-anisidine with ethyl benzoyl acetate in the presence of either HCl or *p*-TsOH (2 mol %) gave a mixture of the enamines **11** and **12** in an approximately 1:2:1 ratio (Scheme 2). Pyrolysis of each purified enamine, **11** and **12**, gave the desired quinoline **13c** in 44% and 12% yield, respectively. However, pyrolysis of the crude mixture of enamines **11** and **12**, followed by a simple trituration of the products in CH₂Cl₂, allowed for the isolation of the pure 7-methoxy isomer **13c** (without any trace of the 5-methoxy isomer **14**) in 17% overall yield. This modified protocol is particularly amenable to large scale synthesis (>100 g) of the key intermediate **13c**.

The two P3 fragments, (2*S*)-*N*-Boc-amino 6-heptenoic and (2*S*)-*N*-Boc-amino 8-nonenoic acids (**20a** and **20b**, respectively), were prepared as shown in Scheme 3. The synthesis of **20a** was initiated from the commercially available acid **16a**, whereas the 8-nonenoic acid (**16b**) was obtained after a Grignard reaction of the 8-bromo-1-octene (**16c**) with CO₂. Enolization of intermediates **17a** and **17b** with potassium hexamethyldisilazide was followed by asymmetric azidation at the C α position with 2,4,6-triisopropylbenzenesulfonyl azide (trisyl azide), as previously reported by Evans.⁴⁴ Reduction of the azide intermediates **18a** and **18b** with SnCl₂ in methanol gave the corresponding free amines (Scheme 3). These products were then protected as the *tert*-butyl carbamates (Boc) to give intermediates **19a** and **19b** in good overall yields. The final P3 building blocks **20a** and **20b** were obtained in good yields after cleavage of the chiral auxiliary with LiOH (Scheme 3).

For the preparation of each macrocyclic ligand, the appropriate P1, P2 and P3 building blocks were first assembled into an acyclic tripeptide, using standard solution-phase peptide chemistry; as an example, the preparation of the P1–P2 dipeptide **25a** and its conver-

(41) After separation of each P1–P2 diastereomeric fragment by chromatography, each dipeptide was carried (independently) to the corresponding acyclic tripeptide diene and macrocyclic inhibitor. Biological evaluation of the final macrocyclic inhibitors indicated that those derived from the P1 fragment **10a** were significantly less potent than those derived from **10b**, consistent with our previous observation using the enantiomers of vinyl ACCA **9**.¹⁷ For example, in an in vitro enzymatic assay, the macrocyclic compound **26** (derived from dipeptide **24a**) was found to be 40-fold less potent than the corresponding compound **33b**, which was derived from dipeptide **23a**. Furthermore, it was determined that the less polar diastereomer in each dipeptide mixture (i.e., **23a/24a** or **23b/24b**) corresponded to analogues derived from the homoallyl ACCA (1*R*,2*R*)-**10b**. Assignment of the absolute configuration of **10b** was based on analytical and NMR data, as well as the in vitro enzymatic potency the saturated compound **35** (compound **35** is the common product formed from catalytic hydrogenations of either **34a**, **34b**, or **36b**).

(42) Poupert, M.-A.; Cameron, D. R.; Chabot, C.; Ghire, E.; Goudreau, N.; Goulet, S.; Poirier, M.; Tsantrizos, Y. S. *J. Org. Chem.* **2001**, *66*, 4743.

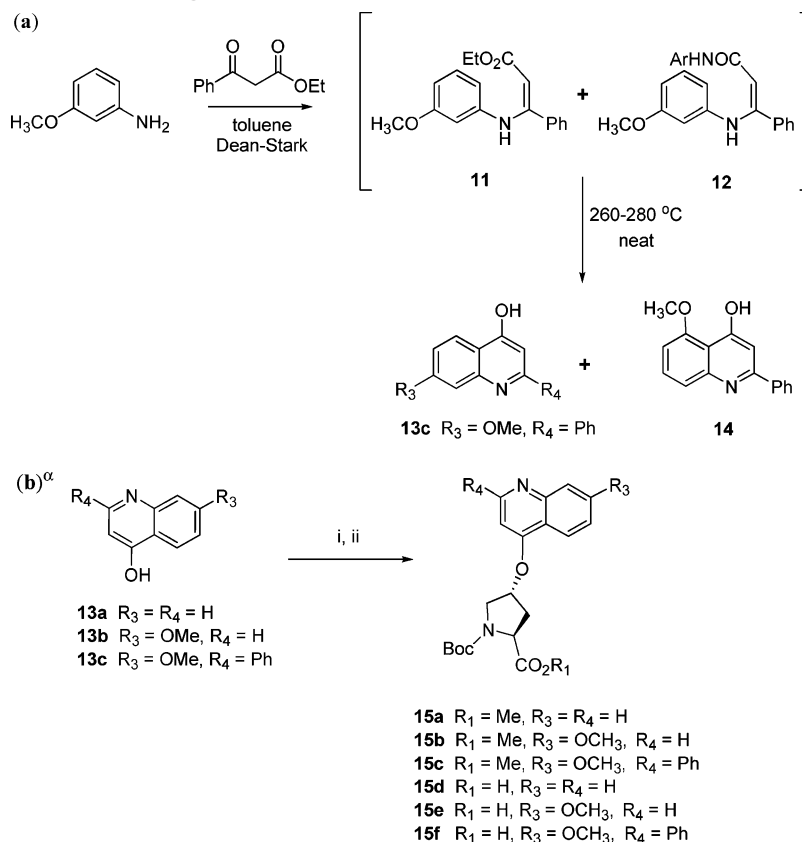
(43) (a) Venturella, P.; Bellino, A. *J. Heterocycl. Chem.* **1975**, *12*, 669. (b) Giardina, G. A. M.; Sarau, H. M.; Farina, C.; Medhurst, A. D.; Grugni, M.; Raveglia, L. F.; Schmidt, D. B.; Rigolio, R.; Luttmann, M.; Vecchiotti, V.; Hay, D. W. P. *J. Med. Chem.* **1997**, *40*, 1794.

(44) (a) Evans, D. A.; Evrard, D. A.; Rychnovsky, S. D.; Fröh, T.; Whittingham, W. G.; DeVries, K. M. *Tetrahedron Lett.* **1992**, *33*, 1189. (b) The % ee of **20a** and **20b** was not determined at this stage, however, upon coupling of these compounds with the P1–P2 dipeptides only one product could be observed by HPLC and NMR, confirming the high enantiomeric purity of the P3 fragments.

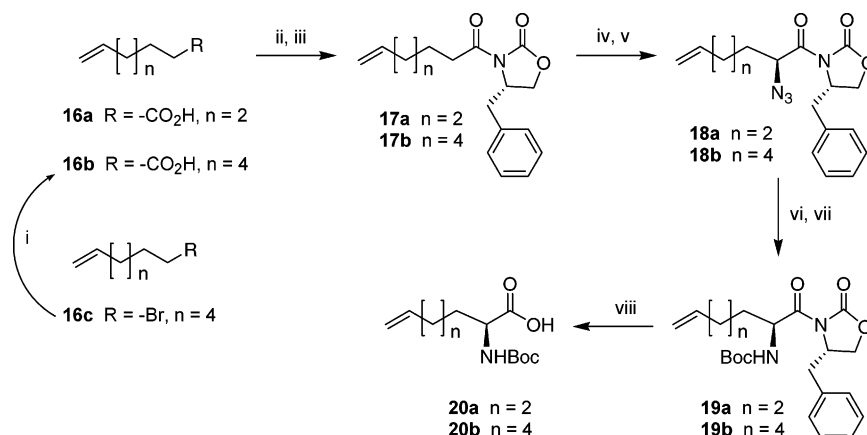
(38) Baldwin, J. E.; Adlington, R. M.; Rawlings, B. J. *Tetrahedron Lett.* **1985**, *26*, 481.

(39) Gassman, P. G.; Schenk, W. N. *J. Org. Chem.* **1977**, *42*, 918.

(40) Capson, T. L.; Poulter, C. D. *Tetrahedron Lett.* **1984**, *25*, 3515.

SCHEME 2. Synthesis of the P2 Fragments 15^a

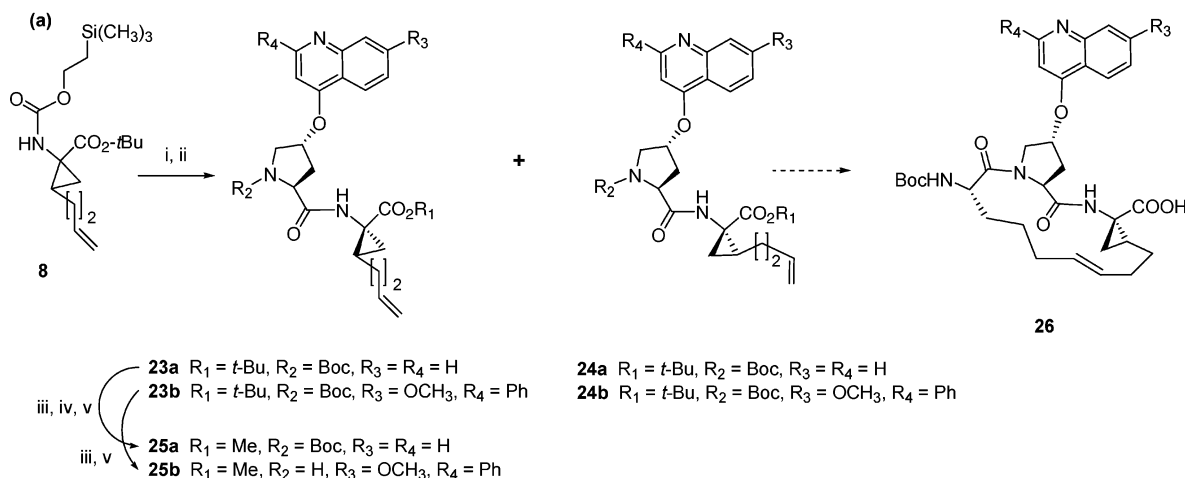
^a Reagents and conditions: (i) *N*-Boc-protected *cis*-4-hydroxyproline, PPh₃, DIAD, THF, rt; (ii) LiOH, H₂O/THF/MeOH, rt.

SCHEME 3. Synthesis of P3 Amino Acid Linkers 20a and 20b^a

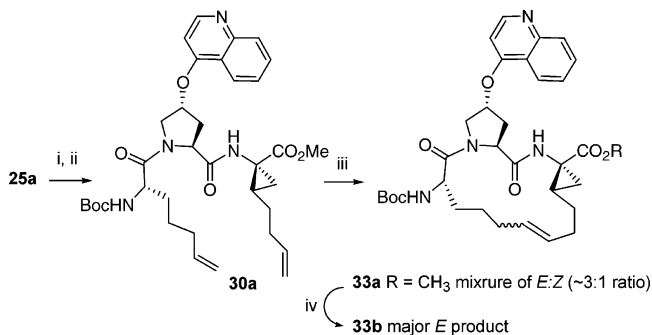
^a Reagents and conditions: (i) Mg, CO₂; (ii) Et₃N, (CH₃)CCOCl, THF, -78 to 0 °C; (iii) *n*-BuLi, 4(*S*)-4-(phenylmethyl)-2-oxazolidinone lithium salt, THF, -78 °C (68%); (iv) KHMDS, THF, -78 °C; (v) trisyl azide, THF, -78 °C (67%); (vi) SnCl₂, MeOH, 0 °C; (vii) Boc₂O, NaHCO₃, dioxane, H₂O (60%); (viii) H₂O₂, LiOH, THF, H₂O, 0 °C (70%).

sion to the macrocyclic ligand **33b** are shown in Schemes 4 and 5, respectively. Peptide coupling reactions were typically carried out in CH₂Cl₂ or DMF, using HATU or TBTU as the coupling agent and DIPEA or NMM as the base. The crude hydrochloride salts of the P1 moieties **5**, **6**, and (1*R*,2*S*)-**9** (obtained after hydrolysis of the Boc protecting group with HCl in dioxane) were coupled directly with one of the P2 fragments **15** to give the *N*-Boc-protected dipeptides **21**, **22**, and **27**, respectively, with average yields of 75–85%. For the synthesis of

dipeptides **23** and **24**, the racemic intermediate **8** was first treated with TBAF and then coupled directly with one of the P2 derivatives **15a** or **15c** (Scheme 4). In each case, the diastereomeric mixture of the corresponding *N*-Boc-protected *tert*-butyl esters **23a,b** and **24a,b** was separated by flash column chromatography and then treated with 4 N HCl in dioxane to simultaneously remove the *N*-Boc protecting group and hydrolyze the *tert*-butyl esters (Scheme 4).⁴¹ Each compound was then treated with diazomethane to reprotect the carboxylic

SCHEME 4. Synthesis of P1–P2 Dipeptides from the Racemic Homoallyl ACCA Derivative 8^a

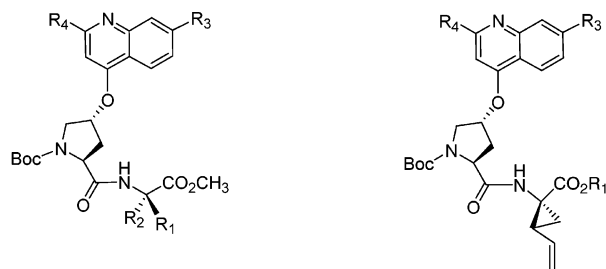
^a Reagents and conditions: (i) TBAF, THF, rt; (ii) **15**, HATU, DIPEA, CH_2Cl_2 , rt; (iii) 4 N HCl dioxane; (iv) Boc_2O , NaHCO_3 , dioxane/ H_2O ; (v) CH_2N_2 , MeOH, CH_2Cl_2 .

SCHEME 5. Synthesis of Macrocyclic Inhibitor 33b^a

^a Reagents and conditions: (i) 4 N HCl–dioxane; (ii) **20a**, HATU, NMM, CH_2Cl_2 , rt; (iii) bis(tricyclohexylphosphine)benzylidene ruthenium(IV) dichloride, CH_2Cl_2 , reflux; (iv) LiOH, H_2O , MeOH, rt.

acid moiety as the methyl ester. The diastereomerically pure dipeptides were then used independently for the synthesis of macrocyclic inhibitors.⁴¹ For the purpose of this study, only dipeptides **25a** and **25b**, which are derived from the P1 moiety (1*R*, 2*R*)-**10b**, will be discussed in detail.⁴¹ However, the macrocyclic peptides derived from **10a** (e.g., compound **26**) were also investigated and found to be weak inhibitors for the HCV NS3 protease.⁴¹

Coupling of each P1–P2 dipeptide with one of the P3 linker moieties (**20a** or **20b**) was carried out under



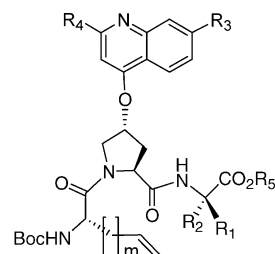
21a $R_1 = \text{CH}_2\text{CH}=\text{CH}_2$, $R_2 = \text{H}$, $R_3 = \text{OCH}_3$, $R_4 = \text{Ph}$

21b $R_1 = \text{H}$, $R_2 = \text{CH}_2\text{CH}=\text{CH}_2$, $R_3 = \text{OCH}_3$, $R_4 = \text{Ph}$

22a $R_1 = \text{CH}_2\text{SCH}_2\text{CH}=\text{CH}_2$, $R_2 = \text{H}$, $R_3 = \text{OCH}_3$, $R_4 = \text{H}$

22b $R_1 = \text{H}$, $R_2 = \text{CH}_2\text{SCH}_2\text{CH}=\text{CH}_2$, $R_3 = \text{OCH}_3$, $R_4 = \text{H}$

27 $R_1 = \text{Et}$, $R_3 = \text{OCH}_3$, $R_4 = \text{Ph}$



28a $R_1 = \text{CH}_2\text{CH}=\text{CH}_2$, $R_2 = \text{H}$, $R_3 = \text{OCH}_3$, $R_4 = \text{Ph}$, $R_5 = \text{Me}$, $m = 5$

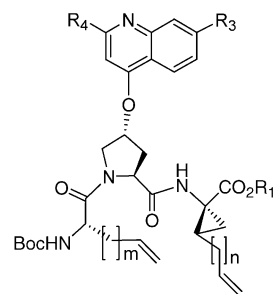
28b $R_1 = \text{H}$, $R_2 = \text{CH}_2\text{CH}=\text{CH}_2$, $R_3 = \text{OCH}_3$, $R_4 = \text{Ph}$, $R_5 = \text{Me}$, $m = 5$

29a $R_1 = \text{CH}_2\text{SCH}_2\text{CH}=\text{CH}_2$, $R_2 = \text{H}$, $R_3 = \text{OCH}_3$, $R_4 = \text{H}$, $R_5 = \text{Me}$, $m = 3$

29b $R_1 = \text{H}$, $R_2 = \text{CH}_2\text{SCH}_2\text{CH}=\text{CH}_2$, $R_3 = \text{OCH}_3$, $R_4 = \text{H}$, $R_5 = \text{Me}$, $m = 3$

29c $R_1 = \text{CH}_2\text{SCH}_2\text{CH}=\text{CH}_2$, $R_2 = \text{H}$, $R_3 = \text{OCH}_3$, $R_4 = \text{H}$, $R_5 = \text{H}$, $m = 3$

29d $R_1 = \text{H}$, $R_2 = \text{CH}_2\text{SCH}_2\text{CH}=\text{CH}_2$, $R_3 = \text{OCH}_3$, $R_4 = \text{H}$, $R_5 = \text{H}$, $m = 3$



30a $R_1 = \text{Me}$, $R_3 = R_4 = \text{H}$, $n = 2$, $m = 3$

30b $R_1 = \text{H}$, $R_3 = R_4 = \text{H}$, $n = 2$, $m = 3$

30c $R_1 = \text{Me}$, $R_3 = \text{OMe}$, $R_4 = \text{Ph}$, $n = 2$, $m = 3$

31 $R_1 = \text{Et}$, $R_3 = \text{OMe}$, $R_4 = \text{Ph}$, $n = 0$, $m = 5$

standard condition to give the acyclic, tripeptide dienes **28** (a,b), **29** (a,b), **30** (a,c), and **31**. Cyclization of each diene under ring-closing metathesis (RCM) conditions, catalyzed by Grubbs' catalyst $(\text{PCy}_3)_2\text{Cl}_2\text{Ru}=\text{CHPh}$,⁴⁵ led to the desired 15-membered ring macrocyclic peptides in good to excellent yields (50–95% yield);⁴⁶ a typical example is shown in Scheme 5. For each compound, the formation of the *Z* or *E* double bond, or a mixture of both, was confirmed by ¹H NMR. Diene **31** derived from the

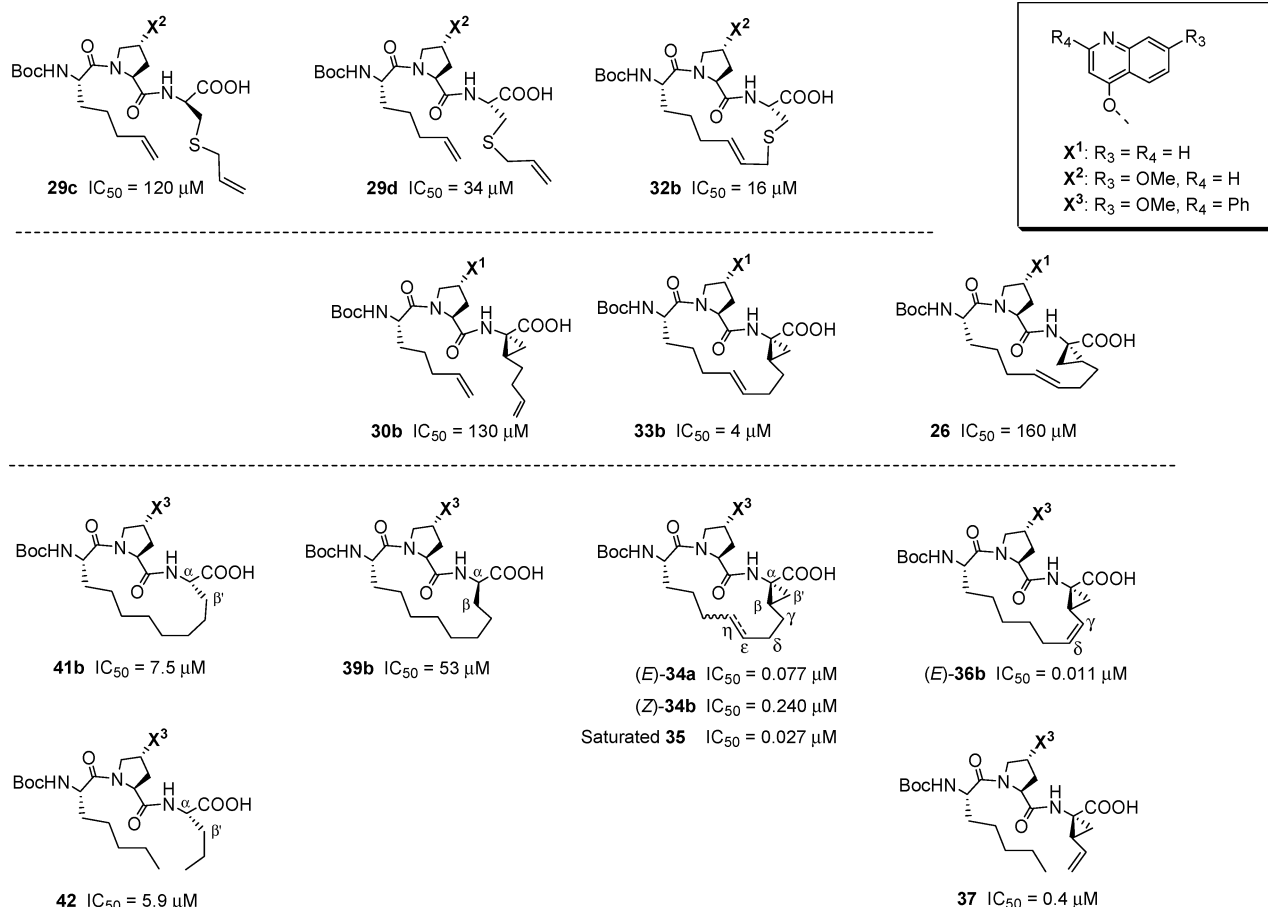


FIGURE 2. Structure–activity of HCV NS3 protease inhibitors: IC_{50} average values from a minimum of three independent in vitro assays, using the full-length NS3–NS4A heterodimer protein of hepatitis C genotype 1b.

rigid vinyl ACCA moiety (1*R*, 2*S*)-**9** formed exclusively [$>98\%$ of the crude macrocyclic product(s)] the *Z* isomer (compounds **36a**), whereas the conformationally flexible allylglycine (**28**), allylcysteine (**29**) and homoallyl ACCA (**30**) analogues gave mixtures of *Z* and *E* macrocyclic products. The *Z/E* ratio depended mostly on the stereochemistry and conformational rigidity of the P1 moiety (although other factors contributed to a lesser extent⁴⁶). For example, the allylglycine derivative **28a** gave a mixture of *Z/E* products in a 1:1 ratio, whereas its diastereomer **28b** gave a ratio of approximately 1:14 (*Z/E*, respectively). The homoallyl ACCA derivative **30c** (having the allyl side chain in the same orientation as **28a** and the same P2 quinoline) gave a *Z/E* ratio of 1:3. Finally, saponification of all ester derivatives (macrocyclic products, as well as the key diene precursors required for SAR studies) under basic conditions, followed by C_{18} , reversed-phase HPLC purification, led to the isolation of all compounds in high purity. These final products were evaluated for their ability to inhibit the HCV NS3 protease (Figure 2), using the in vitro assay described previously.¹⁷ In addition, to evaluate the role of the

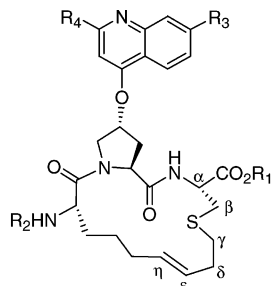
hydrocarbon linker connecting P1 to P3 and confirm the stereochemistry of fragment **10b**, the macrocyclic compounds **34a**, **34b**, and **36b** were independently reduced under catalytic hydrogenation conditions. As expected, all three of these starting materials led to the same saturated product, compound **35**, confirming that the stereochemistry of the homoallyl ACCA fragment **10b** was identical to that of the vinyl ACCA (1*R*,2*S*)-**9**.^{37b,41} Finally, to fully validate the impact of the macrocyclic scaffold, the linear tripeptides **37** and **42**, which correspond directly to inhibitors **36b** and **41b** (respectively) with a single σ -bond disconnection, were prepared and tested in the same enzymatic assay (Figure 2).

Structure–Activity Relationship (SAR). In vivo, a P1 cysteine residue is the dominant determinant for recognition and cleavage efficiency by the NS3 protease at three out of the four cleavage sites along the HCV polyprotein.²⁶ Therefore, in vitro SAR evaluation was initiated with the thia-macrocyclic ligand **32b** containing an S-cysteine residue at P1. Disappointingly, this ligand (**32b**) was only 2-fold more potent than its acyclic precursor **29d**, whereas the latter was approximately 3-fold more potent than its unnatural epimer **29c** (Figure 2).

However, consistent with previous SAR studies,¹¹ macrocyclic derivatives having a cyclopropane moiety at P1 were found to be significantly more potent than ligand **32b**. Compound **33b**, having the least optimum quinoline

(45) (a) Trnka, T. M.; Grubbs, R. H. *Acc. Chem. Res.* **2001**, *34*, 18. (b) Schwab, P.; Grubbs, R. H.; Ziller, J. W. *J. Am. Chem. Soc.* **1996**, *118*, 100. (c) Schwab, P.; France, M. B.; Ziller, J. W.; Grubbs, R. H. *Angew. Chem., Int. Ed. Engl.* **1995**, *34*, 2039.

(46) Other catalysts of the RCM reaction were also evaluated; their effects on yield and the stereochemistry of the resulting macrocyclic product(s) will be published elsewhere.

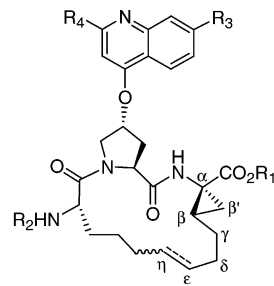


32a $R_1 = \text{CH}_3$, $R_2 = \text{Boc}$, $R_3 = \text{OCH}_3$, $R_4 = \text{H}$, *E* double bond
32b $R_1 = \text{H}$, $R_2 = \text{Boc}$, $R_3 = \text{OCH}_3$, $R_4 = \text{H}$, *E* double bond

moiety X^1 and an *E* double bond at the same position as **32b** (i.e., at $C_{\epsilon,\eta}$ to the P1 acid) was 4-fold more potent than **32b** and 32-fold more potent than its acyclic precursor **30b** (Figure 2). Optimization of the P2 moiety with the 2-phenyl-4-hydroxy-7-methoxyquinoline (P2 = **15f**), as previously reported,^{17,42,47} led to inhibitor **34a** (also having an *E* double bond at $C_{\epsilon,\eta}$ to the P1 acid) which was over 200-fold and 50-fold more potent than **32b** and **33b**, respectively. Interestingly, the *E* analogue **34a** was 3-fold more potent than the *Z* isomer **34b** and both of these compounds (**34a** and **34b**) were approximately 3-fold and 9-fold, respectively, less potent than their common saturated analogue **35** (Figure 2). These results suggested that the electronic properties (π -character) and rigidification elements of the olefinic moiety did not have a significant impact on the overall stability of the NS3 protease–inhibitor complex. However, the conformation of the P1 to P3 linker moiety (as dictated by an *E* vs Z π - or a σ -bond) played a critical role in the overall beneficial effects of the macrocyclic scaffold.

Previous SAR studies, on acyclic tetrapeptide inhibitors of the HCV NS3 protease, revealed that substitution of the P1 cyclopropyl moiety (ACCA) with a vinyl group provided ~5-fold increase in potency over the corresponding ethyl ACCA derivative.^{37a} Macrocyclic derivatives of vinyl ACCA (1*R*,2*S*)-**9**, such as compound **36b**, were also found to be more potent than the corresponding analogues derived from homoallyl ACCA **10b** (i.e., **34a** and **34b**). However, the effect of the olefinic moiety at $C_{\gamma,\delta}$ to the P1 was less significant in this class of compounds than in the acyclic peptides (~2-fold difference in potency was observed between inhibitor **35** and **36b**, Figure 2). Finally, a drop in potency of approximately 36-fold was observed upon *cleavage* of the linker moiety of inhibitor **36b** to produce the corresponding open-chain analogue **37** (Figure 2), once again, highlighting the value of the macrocyclic scaffold.

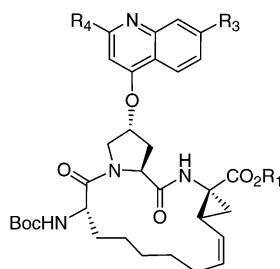
The necessity of the cyclopropyl moiety in providing the optimum molecular recognition and conformation elements between this class of compounds and the HCV NS3 protease was further confirmed by designing a 15-membered ring compound which lacked the β' carbon of the saturated analogue **35**. Compound **39b** was found to be ~2000-fold less potent than **35**, consistent with previous observations with ligand **32b** (Figure 2). It is worth noting that compound **41b**, having the same



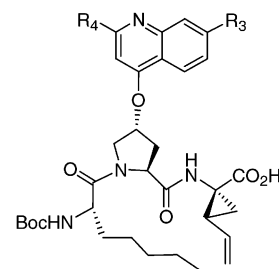
33a $R_1 = \text{CH}_3$, $R_2 = \text{Boc}$, $R_3 = R_4 = \text{H}$, *E* double bond
33b $R_1 = \text{H}$, $R_2 = \text{Boc}$, $R_3 = R_4 = \text{H}$, *E* double bond
33c $R_1 = \text{H}$, $R_2 = \text{Ac}$, $R_3 = R_4 = \text{H}$, *E* double bond

34a $R_1 = \text{H}$, $R_2 = \text{Boc}$, $R_3 = \text{OCH}_3$, $R_4 = \text{Ph}$, *E* double bond
34b $R_1 = \text{H}$, $R_2 = \text{Boc}$, $R_3 = \text{OCH}_3$, $R_4 = \text{Ph}$, *Z* double bond

35 $R_1 = \text{H}$, $R_2 = \text{Boc}$, $R_3 = \text{OCH}_3$, $R_4 = \text{Ph}$, saturated linker



36a $R_1 = \text{CH}_3$, $R_3 = \text{OCH}_3$, $R_4 = \text{Ph}$
36b $R_1 = \text{H}$, $R_3 = \text{OCH}_3$, $R_4 = \text{Ph}$



37

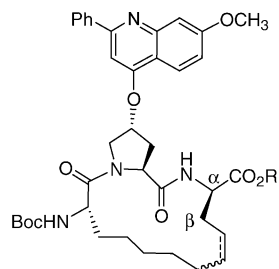
configuration at P1 as the natural substrate(s) of the NS3 protease, is 7-fold more potent than **39b**. However, compound **41b** is almost equipotent to the corresponding acyclic tripeptide **42**, confirming that the difference in potency between **39b** and **41b** is primarily due to the stereochemistry at the C_{α} of P1 and not due to the macrocyclization. These results further validate the essential role of the P1 cyclopropyl moiety and the specific molecular requirements of the target enzyme for which these inhibitors were designed.

Enzyme-Bound Conformation of Ligand 33c and Molecular Modeling of Its Potential Interactions with the Active Site of HCV NS3 Protease. The significant potency differences observed between the macrocyclic inhibitors and their linear precursors provided strong validation for the intuition which led to the design of this novel scaffold. To gain some insight into the NS3-bound conformation of this class of inhibitors, transferred nuclear Overhauser effect (TRNOE) experiments were used to study the structure of inhibitor **33c** in the presence and absence of the enzyme.^{31,48}

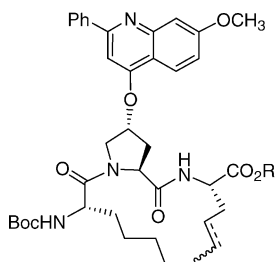
In the absence of the enzyme, very few positive NOEs could be observed in the 2D NOESY spectrum of **33c** (Supporting Information, Figure 1a), consistent with a small molecule tumbling rapidly in solution. In contrast, the NOESY spectrum recorded after the addition of the NS3 protease revealed an extensive set of negative

(47) Goudreau, N.; Cameron, D. R.; Bonneau, P.; Gorys, V.; Plouffe, C.; Poirier, M.; Lamarre, D.; Llinas-Brunet, M. *J. Med. Chem.* **2004**, *47*, 123.

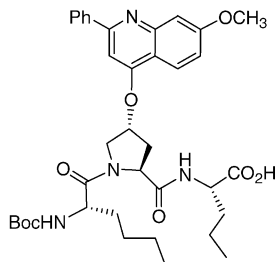
(48) A key condition for studies on protein–ligand interactions using TRNOE experiments is a rapid and reversible exchange between the free and enzyme-bound state of the ligand (the exchange must be faster than the spin–lattice relaxation rate).³¹ The strong binding affinity of compound **33b** for the HCV NS3 protease limited the use of this inhibitor for the TRNOE experiments. This problem was overcome by using the less potent acetate derivative **33c** for the NMR studies.



38 R = CH₃, Z:E (1:1 ratio)
39a R = CH₃, saturated linker
39b R = H, saturated linker

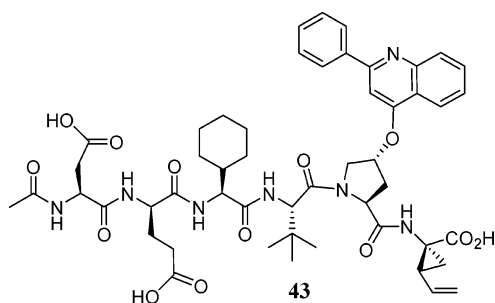


40 R = CH₃, Z:E (1:14 ratio)
41a R = CH₃, saturated linker
41b R = H, saturated linker



42

TRNOE cross-peaks (Supporting Information, Figure 1b), suggesting a reversible and fast exchange between the free in solution and the NS3-bound inhibitor. Furthermore, addition of a more potent competitive inhibitor (hexapeptide **43**; IC₅₀ < 1 nM)⁴⁹ to the preformed NS3/**33c** complex restored the NMR spectrum to that originally observed for the free ligand **33c** (Supporting Information, Figure 1c), confirming that the observed TRNOE cross-peaks originated from the binding of **33c** to the enzyme. This competition experiment provided strong evidence that **33c** was binding specifically to HCV NS3 protease (presumably in, or near, the active site) and could be competitively displaced by the more potent substrate-based inhibitor **43**. Binding of the macrocyclic ligands in the active site of the enzyme was later confirmed by the X-ray crystal structure of analogue **36b** bound to the HCV NS3 protease.¹⁷



43

The distance restraints derived from the volumes of all the TRNOE cross-peaks were then used in a simulated annealing protocol in order to generate an ensemble of

bound conformations. A stereoview of the final 10 lowest energy TRNOE-consistent bound conformations of **33c** are superimposed in Figure 3a. The well-defined ensemble of structures obtained for inhibitor **33c** gave a root-mean-square deviation for the peptidic backbone of only 0.04 Å. Due to some overlapping resonances, leading to some ambiguous TRNOE cross-peaks, the precise bound orientation of the hydrocarbon linker moiety could not be fully determined, however, a restricted range of conformations was reliably proposed (Figure 3a). Consistent with previous observations,^{12,15,47} a strong TRNOE cross-peak was observed between the β and γ pro-R protons of the proline ring suggesting that the quinoline moiety adopted a pseudoaxial conformation relative to the proline ring (Figure 3b). Interestingly, the ROESY NMR data of several macrocyclic compounds (free in solution) was also consistent with the conformation shown in Figure 3, thus indicating that the predominant conformation of the macrocyclic scaffold in the free state was very similar to that of the enzyme-bound complex.

Finally, a model of the inhibitor/enzyme complex was created by docking the NMR-derived structure of **33c** into the active site of the apo NS3 protease.⁵⁰ This complex was first energy-minimized and then submitted to a 1 ns molecular dynamic simulation in a water droplet. The minimized model of the NS3/**33c** complex (Figure 4a) suggested an extensive network of interactions between the inhibitor and the active site of the protease, including hydrogen-bond interactions between the P3 NH and CO groups of **33c** and A157,¹⁶ and between the P1 NH of **33c** and the carbonyl of residue R155.¹⁷ In addition, the carboxylate anion was poised perfectly, allowing for potential interactions with both the oxyanion hole of the protease and H57, while the P1–P3 hydrocarbon linker moiety was docked well within the S1–S3 binding pocket and within van der Waals distance from V132. Based on this model, the P1 cyclopropyl moiety of the ligand would also be expected to form beneficial interactions with the F154 residue at the floor of the S1 binding pocket (Figure 4a). The difference in the π-character between a P1 vinyl ACCA moiety and a P1 ethyl ACCA moiety may account for the modest potency difference observed between analogues such as **36b** and **35** (Figure 2). It is interesting to note that although this model predated our cocrystal structure of inhibitor **36b** bound to the NS3/4A_{peptide} protease domain,¹⁷ it provided valuable structural information with remarkable accuracy. In Figure 4b, the NMR-derived bound conformation of **33c** and the crystal structure of **36b** are superimposed; a root-mean-square deviation for their P1–P3 backbone atoms of 0.32 Å was calculated.

Conclusions

We have undertaken the challenge of trying to understand the subtle details governing the interactions between the HCV NS3 serine protease and its polyprotein

(49) Pause, A.; Kukolj, G.; Bailey, M.; Brault, M.; Dô, F.; Halmos, T.; Lagacé, L.; Maurice, R.; Marquis, M.; Mckercher, G.; Pellerin, C.; Pilote, L.; Thibault, D.; Lamarre, D. *J. Biol. Chem.* **2003**, *278*, 20374.

(50) (a) Yan, Y.; Li, Y.; Munshi, S.; Sardana, V.; Cole, J. L.; Sardana, M.; Steinkühler, C.; Tomei, L.; De Francesco, R.; Kuo, L. C.; Chen, Z. *Protein Science* **1998**, *7*, 837. (b) Kim, J. L.; Morgenstern, K. A.; Lin, C.; Fox, T.; Dwyer, M. D.; Landro, J. A.; Chambers, S. P.; Markland, W.; Lepre, C. A.; O'Malley, E. T.; Harbeson, S. L.; Rice, C. M.; Murcko, M. A.; Caron, P. R.; Thomson, J. A. *Cell* **1996**, *87*, 343. (c) Love, R. A.; Parge, H. E.; Wickersham, J. A.; Hostomsky, Z.; Habuka, N.; Moomaw, E. W.; Adachi, T.; Hostomska, Z. *Cell* **1996**, *87*, 331.

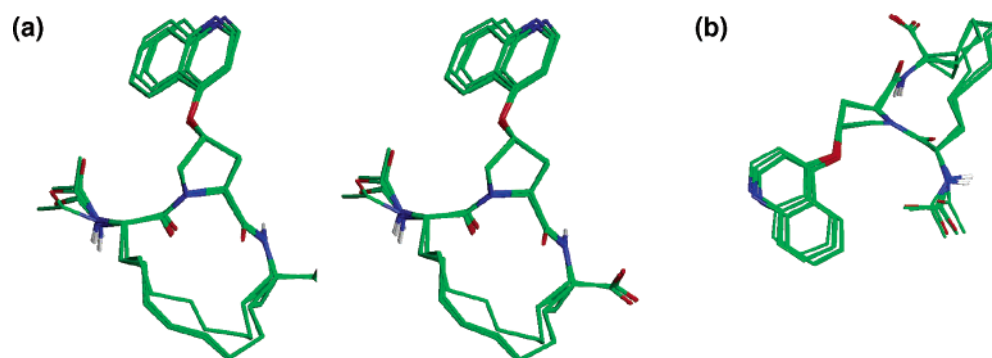


FIGURE 3. (a) Stereoview of the superposition (P1–P3 backbone atoms only) of the 10 best structures generated by restrained simulated annealing and derived from the NMR data of inhibitor **33c** when bound to the NS3 protease. The structures are colored by atom type: oxygen in red, nitrogen in blue, carbon in green, and hydrogen in gray (most of the hydrogen atoms are not shown). (b) Side view of the 10 best NMR-derived NS3-bound structures of **33c**.

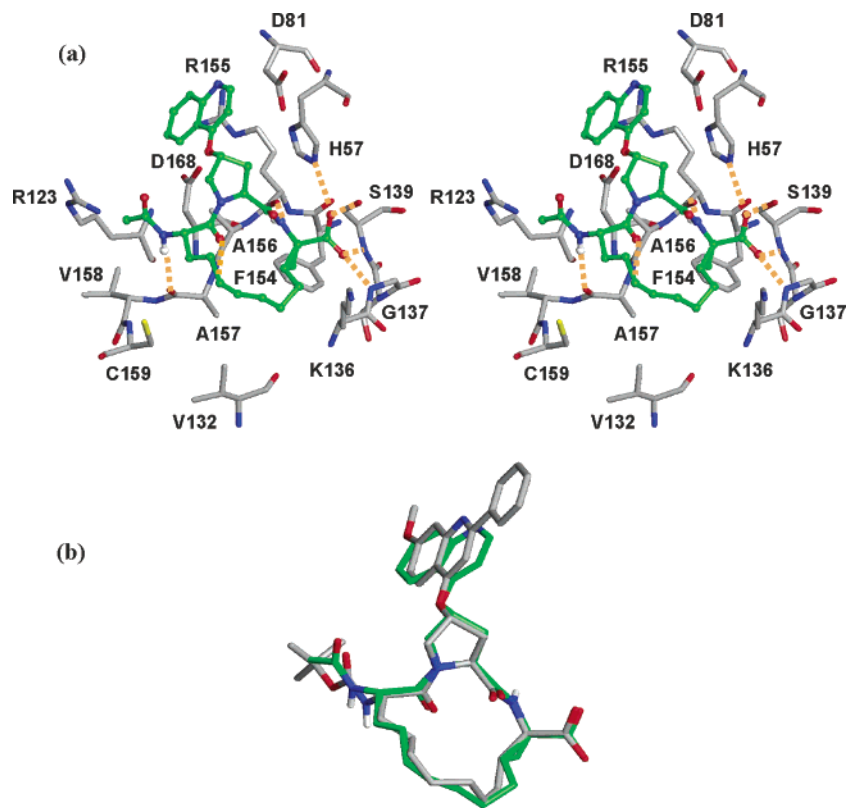


FIGURE 4. (a) Model of the NS3-bound inhibitor **33c**; key interactions that may be implicated in hydrogen bonds with the active-site residues (as suggested by the model) are indicated with dashed orange lines. Carbon atoms of the inhibitor are colored in green, those of the NS3 protein in gray. All nitrogen atoms and oxygen atoms are colored in blue and red, respectively. The sulfur atom of C159 is colored in yellow. (b) Comparison of the NMR-derived bound structure of **33c** (molecule in green) to the cocrystal structure of **36b** (molecule in gray) bound to the active site of the NS3/NS4A_{peptide} protease domain. The two structures were superimposed using the P1–P3 backbone atoms only with a root-mean-square deviation of 0.32 Å.

substrate. Some key molecular recognition elements of substrate-based acyclic peptides were evaluated by NMR and computational chemistry in order to design β -strand mimics which are potent inhibitors of the NS3 protease. Efficient protocols were developed, which allowed for the rapid synthesis of macrocyclic analogues addressing the role of the P1 moiety and the hydrocarbon linker connecting the P1–P3 side chains. Finally, we demonstrated that the successful design of this unique 15-membered ring scaffold plays a critical role in the strong affinity

that this novel class of ligands exhibit toward the HCV NS3 serine protease.

Experimental Section

General Protocol for Amide Bond Formation. A solution containing the free acid and the free amine fragments (ratio of ~1:1 equiv), in the minimum volume of CH_2Cl_2 or DMF (depending on the solubility of the compounds), HATU (~1.1 equiv) and DIPEA (3 equiv) was stirred at rt for 5–15 h (completion of the reaction was monitored by analytical

HPLC).⁵¹ The reaction mixture was then diluted with EtOAc, washed with 5% aqueous NaHCO₃ and brine, dried over anhydrous MgSO₄, concentrated under reduced pressure, and purified by flash column chromatography.

General Protocol for RCM. The diene starting material was dissolved in CH₂Cl₂ at a concentration of 0.01 M, and the solution was deoxygenated by bubbling argon (~1 h for a volume of 500 mL). A solution of Grubbs' catalyst bis(tricyclohexylphosphine)benzylideneruthenium(IV) dichloride (5 mmol % dissolved in a small amount of degassed CH₂Cl₂) was added, and the reaction mixture was stirred under reflux for ~2 h (completion of the reaction was monitored by analytical HPLC). The crude reaction mixture was subsequently concentrated under reduced pressure and filtered through a short pad of silica gel, eluting first with CH₂Cl₂ (to remove most of the catalyst) and then with EtOAc to isolate the macrocyclic product(s) in reasonable purity (>80% homogeneity by HPLC). In some cases, the desired macrocyclic compound(s) was further purified by flash column chromatography to obtain the ester(s) in very high purity (>98% homogeneity) and 50–95% isolated yield. However, most of the time, the semipure macrocyclic ester was used directly in the final hydrolysis reaction.

General Protocol for Ester Hydrolysis and Purification of Inhibitors. Saponification of all esters was carried out under basic conditions using LiOH (2.5 equiv) in a solution of THF/MeOH/H₂O and over a period of 16 h at rt. The reaction mixture was then acidified to pH = 4 using 1 N HCl and evaporated to dryness under reduced pressure to obtain the free acids. Intermediate building blocks were used in the subsequent synthetic steps without further purification. However, all compounds used for evaluation in the enzymatic in vitro assay were purified to >95% homogeneity by semi-preparative C₁₈ reversed-phase HPLC using a solvent gradient from 5% to 100% aqueous CH₃CN (all solvents contained 0.06% TFA). The final homogeneity of each inhibitor was determined by analytical HPLC using either method A or B. Method A: Vydac C₁₈ reversed-phase column (0.46 × 12.5 cm i.d., 5 μm, 300 Å) and a 35 min linear gradient from 0 to 100% aqueous CH₃CN (all solvents contained 0.06% TFA) at a flow rate of 1.5 mL/min with the UV detector set at λ = 230 nm. Method B: The UV detector was set simultaneously at λ = 220 and 254 nm. Solvent A = 5% aqueous CH₃CN, solvent B = 100 CH₃CN, both solvents contained 0.06% TFA. YMC Combiscreen ODS-AQ C₁₈ reversed-phase column (50 × 4.6 mm i.d., S-5 μm, 12 nm) with linear gradient from solvent A to 1:1 mixture of solvents A/B at a flow rate of 3 mL/min for the first 6 min. After that period, the flow rate was increased to 3.5 mL/min, and the solvent gradient was changed from 1:1 A/B to 100% B over a period of 4.5 min.

D-Allylglycine Methyl Ester Hydrochloride (5a). To an ice-cold solution of anhydrous methanol (14.5 mL) was added thionyl chloride (1.9 mL, 26 mmol) dropwise. To this solution was added d-allylglycine (970 mg, 8.43 mmol) in small portions. The resulting solution was stirred at rt for 4 h and then at reflux for 2.5 h. After cooling, the reaction mixture was concentrated under reduced pressure to afford compound **5a** as a white solid (1.40 g, >99% yield): ¹H NMR (DMSO-*d*₆) δ 2.59 (dd, *J* = 7 Hz, 2H), 3.71 (s, 3H), 4.08 (bs, 1H), 5.21–5.10 (m, 2H), 5.82–5.72 (m, 1H), 8.70 (bs, 3H); ES⁺ MS *m/z* 130 (M + H)⁺.

D-S-Allylcysteine Methyl Ester Hydrochloride (6a). D-Cysteine hydrochloride (290 mg, 1.6 mmol) was mixed with allyl bromide (300 mg, 2.20 μL, 2.5 mmol) in 2 M NH₄OH (5 mL) and stirred at rt for 20 h. The reaction mixture was concentrated to precipitate the product as a white solid. The solid was filtered, washed with ethanol (3 × 5 mL), dried under reduced pressure, and used in the following step without

further purification: ¹H NMR (DMSO-*d*₆) δ 2.66 (dd, *J* = 8.6, 14.0 Hz, 1H), 2.95 (dd, *J* = 3.7, 14.0 Hz, 1H), 3.12–3.21 (m, 2H), 3.28 (dd, *J* = 3.8, 14.0 Hz, 1H), 5.08 (dd, *J* = 1.6, 9.9 Hz, 1H), 5.17 (dd, *J* = 1.6, 16.9 Hz, 1H), 5.71–5.81 (m, 1H), 7.50 (bs, 2H).

The 3-allylsulfanyl-2-aminopropionic acid intermediate (72 mg, 0.45 mmol) was subsequently mixed with Boc₂O (110 mg, 0.49 mmol) and K₂CO₃ (1 M, 560 μL, 0.56 mmol) in THF (5 mL) and stirred at rt for 20 h. H₂O was added and the reaction mixture was concentrated under reduced pressure to remove most of the THF. The aqueous mixture was extracted with Et₂O (2 × 20 mL) to remove any unreacted Boc₂O, acidified to pH ~3 with acetic acid and re-extracted with EtOAc (2 × 20 mL). The combined organic layers were washed with brine, dried over anhydrous MgSO₄, filtered, and evaporated to give the Boc-protected 3-allylsulfanyl-2-aminopropionic acid intermediate as a white solid (~120 mg) which was used in the following step without purification: ¹H NMR (CDCl₃) δ 1.46 (s, 9H), 2.87–3.02 (m, 2H), 3.16 (d, *J* = 7.0 Hz, 2H), 4.54 (bs, 1H), 5.12 (s, 1H), 5.16 (d, *J* = 4.8 Hz, 1H), 5.35 (bd, *J* = 5.7 Hz, 1H), 5.71–5.82 (m, 1H).

The above *N*-Boc acid was treated with CH₂N₂ in CH₂Cl₂ until the yellow color of the diazomethane persisted. The solution was evaporated to dryness to give the *N*-Boc-protected derivative of **6a** as a white solid (~125 mg): ¹H NMR (CDCl₃) δ 1.45 (s, 9H), 2.79–2.92 (m, 2H), 3.12–3.15 (m, 2H), 3.77 (s, 3H), 4.52 (bs, 1H), 5.11 (bs, 1H), 5.14 (bs, 1H), 5.30 (bs, *J* = 1H), 5.70–5.81 (m, 1H).

After hydrolysis of the Boc protecting groups with HCl in dioxane (~30 equiv) the P1 fragment d-S-allylcysteine methyl ester hydrochloride (**6a**) was isolated [ES⁺ MS *m/z* 176 (M + H)⁺; ES[−] MS *m/z* 174 (M − H)[−]] and used immediately for the synthesis of the dipeptide P1–P2 intermediate **20a**.

Intermediate 7a. To a suspension of benzyltriethylammonium chloride (5.08 g, 22.3 mmol) in 50% aqueous NaOH (50 mL), 1,2-dibromo-5-hexene (8.10 g, 33.46 mmol), and di-*tert*-butylmalonate (4.82 g, 22.30 mmol) were added in succession. The mixture was stirred vigorously at rt for 16 h, diluted with H₂O, and extracted with CH₂Cl₂ (3 × 50 mL). The combined organic layers were further washed with H₂O (2 × 50 mL) and brine/H₂O (2/1, 2 × 50 mL), dried over anhydrous MgSO₄, and evaporated to dryness under vacuum. The crude residue was purified by flash column chromatography on silica gel, using a gradient from 3% to 5% EtOAc in hexanes as the eluent to obtain compound **7a** in 38% yield (2.48 g): ¹H NMR (CDCl₃) δ 1.19 (bd, *J* = 7.9 Hz, 2H), 1.25–1.33 (m, 1H), 1.46 (s, 9H), 1.48 (s, 9H), 1.47–1.60 (m, 1H), 1.75–1.82 (m, 1H), 2.14–2.22 (m, 2H), 4.93–5.50 (m, 1H), 4.96 (dm, *J* = 10.2 Hz, 1H), 5.18 (dm, *J* = 17.2 Hz, 1H); ES⁺ MS *m/z* 297 (M + H)⁺.

Intermediate 7b. To a suspension of potassium *tert*-butoxide (5.75 g, 51.25 mmol) in anhydrous diethyl ether (150 mL) at 0 °C was added H₂O (203 μL, 11.27 mmol), and the reaction mixture was stirred at 0 °C for 10 min. An ether solution of compound **7a** (2.48 g in 10 mL diethyl ether, 10.25 mmol) was added, and the mixture was stirred at rt for 5 h. The mixture was diluted with ice-cold H₂O and extracted with diethyl ether (3 × 200 mL). The aqueous layer was acidified to pH ~3.5 with ice-cold 10% aqueous citric acid and re-extracted with EtOAc (3 × 200 mL). The combined EtOAc layers were washed with H₂O (2 × 100 mL) and brine (100 mL), dried over anhydrous MgSO₄, and evaporated to give compound **7b** in 85% yield (based on some recovered starting material): ¹H NMR (400 MHz, CDCl₃) δ 1.51 (s, 9H), 1.64–1.68 (m, 1H), 1.68–1.75 (m, 1H), 1.77–1.88 (m, 1H), 1.96–2.01 (m, 1H), 2.03–2.22 (m, 3H), 5.01 (dm, *J* = 6.4 Hz, 1H), 5.03 (dm, *J* = 14.9 Hz, 1H), 5.72–5.83 (m, 1H); ES⁺ MS *m/z* 241 (M + H)⁺.

Intermediate 8. To a solution of the acid **7b** in anhydrous benzene (1.14 g in 25 mL benzene, 4.74 mmol) was added Et₃N (800 μL, 5.68 mmol) followed by the addition of diphenylphosphoryl azide (1.13 mL, 5.21 mmol), and the mixture was heated to reflux for 3.5 h. Subsequently, trimethylsilylethanol (1.36

(51) In most cases, the choice of the coupling reagent and the base was not critical to the efficiency of coupling; replacement of HATU/DIPEA with TBTU/DIPEA or HATU/NMM gave very similar results.

mL, 9.48 mmol) was added, and stirring at reflux was continued for an additional 4 h. The mixture was then cooled to rt, evaporated to half of its original volume, diluted with diethyl ether (30 mL), washed with 5% aqueous NaHCO_3 (2×30 mL) and brine (50 mL), dried over anhydrous MgSO_4 , and evaporated. The residual oil was chromatographed on silica gel using 10% EtOAc in hexanes as the eluent to obtain pure compound **8** in 88% yield (1.49 g): ^1H NMR (CDCl_3) δ 0.03 (s, 9H), 0.91–0.99 (m, 2H), 1.18–1.29 (m, 2H), 1.45 (bs, 11H), 1.56–1.72 (m, 2H), 2.02–2.18 (m, 2H), 4.12 (t, $J = 8.3$ Hz, 2H), 4.93 (dm, $J = 10.2$ Hz, 1H), 4.98 (dm, $J = 17.2$ Hz, 1H), 5.07 (bs, 1H), 5.71–5.83 (m, 1H); ES^+ MS m/z 356.4 ($\text{M} + \text{H}^+$).

4-Hydroxy-7-methoxy-2-phenylquinoline (13c). A solution of ethyl benzoyl acetate (100.0 g, 0.52 mol), *m*-anisidine (128.1 g, 1.04 mol), and 4 N HCl/dioxane (5.2 mL) in toluene (1.0 L) was refluxed for 6.25 h in a Dean–Stark apparatus. The cooled toluene solution was successively washed with aqueous 10% HCl (2×300 mL), 1 N NaOH (2×300 mL), H_2O (300 mL), and brine (150 mL). The toluene phase was dried over anhydrous MgSO_4 , filtered, and concentrated under vacuum to give a 1.2:1.0 mixture of enamine ester **11** and enamine amide **12** (total 144.6 g of material, 45% and 38% crude yield of **11** and **12**, respectively) as a dark brown oil. The crude oil was heated to 280 °C for 80 min while the EtOH generated from the reaction was distilled. The cooled dark solid obtained was triturated with CH_2Cl_2 (200 mL). The suspension was filtered and the resulting solid washed with CH_2Cl_2 to give the desired quinoline **13c** (22.6 g, 17% overall yield from *m*-anisidine) as a beige solid:

Enamine ester 11: ^1H NMR ($\text{DMSO}-d_6$) δ 1.22 (t, $J = 7.0$ Hz, 3H), 3.51 (s, 3H), 4.13 (q, $J = 7.0$ Hz, 2H), 4.93 (s, 1H), 6.27–6.25 (m, 2H), 6.48 (dd, $J = 8.1$, 1.9 Hz, 1H), 6.99 (t, $J = 8.1$ Hz, 1H), 7.41–7.35 (m, 5H), 10.13 (s, 1H); ^{13}C NMR ($\text{DMSO}-d_6$) δ 14.4, 54.8, 59.0, 91.3, 107.4, 108.8, 114.1, 127.9, 128.7, 129.4, 129.7, 135.6, 141.3, 158.3, 159.4, 168.9; ES^+ MS m/z 298 ($\text{M} + \text{H}^+$).

Enamine amide 12: ^1H NMR ($\text{DMSO}-d_6$) δ 3.52 (s, 3H), 3.72 (s, 3H), 5.22 (s, 1H), 6.19 (bs, 1H), 6.24 (bd, $J = 8.1$ Hz, 1H), 6.43 (dd, $J = 8.1$, 2.0 Hz, 1H), 6.59 (dd, $J = 8.0$, 1.5 Hz, 1H), 6.99 (t, $J = 8.1$ Hz, 1H), 7.12 (bd, $J = 8.0$ Hz, 1H), 7.18 (t, $J = 8.0$ Hz, 1H), 7.35 (bs, 1H), 7.42–7.36 (m, 5H), 9.84 (s, 1H), 10.83 (s, 1H); ^{13}C NMR ($\text{DMSO}-d_6$) δ 54.7, 54.9, 96.3, 104.6, 106.7, 108.0, 108.1, 111.2, 113.5, 127.6, 128.7, 129.4, 129.5, 136.4, 140.8, 142.0, 155.4, 159.4, 159.5, 167.7; ES^+ MS m/z 375 ($\text{M} + \text{H}^+$).

Quinoline 13c (7-methoxy quinoline isomer): ^1H NMR ($\text{DMSO}-d_6$) δ 3.86 (s, 3H), 6.25 (s, 1H), 6.93 (dd, $J = 2.0$, 9.0 Hz, 1H), 7.20 (d, $J = 2.0$ Hz, 1H), 7.59–7.55 (m, 3H), 7.83–7.78 (m, 2H), 7.99 (d, $J = 9.0$ Hz, 1H), 11.51 (s, 1H); ^{13}C NMR ($\text{DMSO}-d_6$) δ 55.4, 99.7, 107.1, 113.2, 119.2, 126.5, 127.2, 129.0, 130.4, 134.2, 142.3, 149.6, 161.9, 176.5; ES^+ MS m/z 252 ($\text{M} + \text{H}^+$).

Synthesis of the P2 Building Blocks 15f. A solution of Boc-protected *cis*-4-hydroxyproline, the desired 4-hydroxyquinoline (**13c**, 1 equiv), and Ph_3P (2 equiv) in anhydrous THF (~70 mM concentration) was cooled to 0 °C. Diisopropyl azodicarboxylate (DIAD, 2 equiv) was added dropwise, and the reaction mixture was stirred at rt for approximately 15 h. After that period, the reaction mixture was evaporated to dryness under vacuum, and the residue was purified by flash column chromatography to give the methyl ester **15c** in typically 70–80% yield and reasonably good purity. Complete removal of the Ph_3P -PO by flash column chromatography was often difficult. However, an easily removable phosphine reagent was recently reported which allowed for the synthesis of intermediate of such intermediates in higher yields and excellent purity.⁵² The methyl ester **15c** was hydrolyzed under the usual basic conditions. The reaction suspension was poured into H_2O , the

mixture was extracted with EtOAc, and the aqueous layer was acidified to pH ~4. The free acid **15f** precipitated from the acidic aqueous layer as a white solid, which was filtered and dried under vacuum before used for the synthesis of P1–P2 fragments: ^1H NMR ($\text{DMSO}-d_6$, rotamers in ~2:1 ratio) δ (major rotamer) 1.36 (s, 9H), 2.32–2.43 (m, 1H), 2.63–2.73 (m, 1H), 3.76 (bs, 2H), 3.93 (s, 3H), 4.34–4.41 (m, 1H), 5.53–5.59 (m, 1H), 7.17 (dd, $J = 9.2$, 2.5 Hz, 1H), 7.39 (d, $J = 2.5$ Hz, 1H), 7.45 (s, 1H), 7.48–7.56 (m, 3H), 8.00 (d, $J = 9.2$ Hz, 1H), 8.27 (d, $J = 7.0$ Hz, 2H); ES^+ MS m/z 465.5 ($\text{M} + \text{H}^+$).

8-Nonenoic Acid (16b). To a stirred suspension of finely cut Mg ribbons (0.55 g, 22.5 mmol) in dry THF (30 mL) containing dibromoethane (0.1 mL) was added dropwise 8-bromo-1-octene (2.52 mL, 15 mmol) over a period of 15 min (the reaction is slightly exothermic). After 30 min, the mixture was heated to 38 °C for 1 h and then cooled to –78 °C before it was added via a cannula onto an excess amount of solid CO_2 . The mixture was diluted with diethyl ether (100 mL), and the solution was washed with brine (2×50 mL), dried over anhydrous MgSO_4 , and evaporated to dryness under vacuum. The crude oil obtained was purified by flash column chromatography on silica gel using 15% EtOAc in hexanes as the eluent to give the carboxylic acid **16b** in 62% yield (1.44 g): ^1H NMR (CDCl_3) δ 1.31–1.42 (m, 6H), 1.60–1.69 (m, 2H), 2.02–2.09 (m, 2H), 2.35 (t, $J = 8.3$ Hz, 2H), 4.99 (dm, $J = 10.0$ Hz, 1H), 5.04 (dm, $J = 17.0$ Hz, 1H), 5.75–5.86 (m, 1H).

Intermediate 17b. To a vigorously stirring solution of the carboxylic acid **16b** (1.36 g, 8.7 mmol) in anhydrous THF (70 mL) at –78 °C were added freshly distilled Et_3N (1.6 mL; 11.3 mmol) and pivaloyl chloride (1.18 mL, 9.58 mmol) via a syringe under anhydrous conditions. The mixture was stirred at –78 °C for 15 min and then at 0 °C for 45 min. The mixture was cooled again to –78 °C and transferred via a cannula into an anhydrous solution of (4*S*)-4-(phenylmethyl)-2-oxazolidinone lithium salt in THF at –78 °C; the lithium salt of the oxazolidinone reagent had been previously prepared by the slow addition of *n*-BuLi (2.00 M in hexanes, 7.85 mL, 15.7 mmol) into a THF (20 mL) solution of the oxazolidinone (2.78 g, 15.7 mmol) in THF at –78 °C. The reaction mixture was stirred at –78 °C for 15 min and then at rt for 1.5 h. Finally, it was quenched with an aqueous solution of sodium bisulfate (1 M, 100 mL), and the THF evaporated to 3/4 of its initial volume under vacuum. The residue was extracted with EtOAc (2×150 mL), the combined organic layers were washed with 5% NaHCO_3 (3×50 mL), brine (2×50 mL), dried over anhydrous MgSO_4 , and evaporated to dryness under vacuum. The resulting crude oil was purified by flash column chromatography (using 15% EtOAc in hexanes) to obtain compound **17b** in 68% yield (1.88 g): ^1H NMR (CDCl_3) δ 1.35–1.47 (m, 6H), 1.67–1.74 (m, 2H), 2.02–2.09 (m, 2H), 2.65 (dd, $J = 13.4$, 9.9 Hz, 1H), 2.84–3.02 (m, 2H), 3.31 (dd, $J = 13.4$, 3.2 Hz, 1H), 4.13–4.22 (m, 2H), 4.62–4.71 (m, 1H), 4.93 (dm, $J = 10.2$ Hz, 1H), 5.00 (dd, $J = 1.6$, 17.2 Hz, 1H), 5.75–5.84 (m, 1H), 7.18–7.38 (m, 5H); ES^+ MS m/z 316.4 ($\text{M} + \text{H}^+$).

Compound 18b. To a stirred solution of KHMDS (0.8 M THF, 22 mL, 17.5 mmol) in dry THF (50 mL) at –78 °C was added a solution of the acid derivative **17b** (3.25 g, 10.30 mmol) in dry THF (40 mL) at –78 °C via a cannula. The reaction mixture was stirred at –78 °C for 45 min, and then a solution of trisyl azide (3.67 g, 11.85 mmol, in 40 mL of dry THF) was added at –78 °C. The mixture was stirred at –78 °C for 3 min and then quenched with acetic acid (5 mL). The mixture was stirred at rt for 2 h and finally at 40 °C for 15 min. Most of the THF was then evaporated under vacuum, and the residue was dissolved in EtOAc (100 mL). This was washed with H_2O (50 mL), 5% NaHCO_3 (3×50 mL), and brine (50 mL), dried over anhydrous MgSO_4 , and evaporated to dryness under vacuum. The oil obtained was purified by flash column chromatography (using 1:1 hexanes/ CH_2Cl_2) to give compound **18b** (2.47 g, yield 67%): ^1H NMR (CDCl_3) δ 1.32–1.45 (m, 5H), 1.45–1.8 (m, 1H), 1.65–1.73, 1.75–1.88 (2m, 2H, rotamers), 2.01–2.11 (m, 2H), 2.72–3.02 (m, 1H), 3.33 (dd, $J = 3.2$, 13.4

(52) Yoakim, C.; Guse, I.; O'Meara, J. A.; Thavonekham, B. *Synlett* **2003**, 473.

Hz, 1H), 4.10–4.28 (m, 2H), 4.62–4.72 (m, 1H), 4.90–5.05 (m, 3H), 5.73–5.88 (m, 1H), 7.17–7.38 (m, 5H); ES⁺ MS *m/z* 357.5 (M + H)⁺.

Compound 19b. To a stirred solution of anhydrous SnCl₂ (2.61 g, 13.8 mmol) in anhydrous MeOH (80 mL) was cannulated a solution of the azide **18b** (2.45 g, 6.9 mmol) at 0 °C in anhydrous MeOH (20 mL). The mixture was stirred at rt for 4 h. The MeOH was evaporated, the foamy material obtained was taken into dioxane/H₂O (100 mL/20 mL) and treated with Boc₂O (3.0 g, 13.8 mmol) and NaHCO₃ (2.89 g, 34.5 mmol), the pH was adjusted to 8 with more NaHCO₃ (if needed), and the mixture was stirred at rt for 16 h. Part of the dioxane was evaporated (~50%), and the residue was extracted with EtOAc (2 × 100 mL). The combined organic layer was washed with brine (2 × 50 mL), dried over anhydrous MgSO₄, and evaporated to dryness. The residue obtained was purified by flash column chromatography (using 20–25% EtOAc in hexanes as eluent) to give the compound **19b** (1.75 g, yield 60%): ¹H NMR (CDCl₃) δ 1.27–1.53 (m, 7H), 1.46 (s, 9H), 1.80 (m, 1H), 2.00–2.08 (m, 2H), 2.80 (t, *J* = 12.1 Hz, 1H), 3.34 (d, 14.3 Hz, 1H), 4.17–4.23 (m, 2H), 4.60–4.66 (m, 1H), 4.93 (d, *J* = 10.2 Hz, 1H), 5.50 (dd, *J* = 1.9, 17.2 Hz, 1H), 5.13 (bs, 1H), 5.38–5.43 (m, 1H), 5.74–5.84 (m, 1H), 7.22–7.36 (m, 5H); ES⁺ MS *m/z* 431.6 (M + H)⁺.

(2S)-N-Boc-2-amino-8-nonenic Acid (20b). To a stirred solution at 90 °C of the *N*-Boc derivative **19b** (1.74 g, 4.04 mmol) in THF/H₂O (75 mL/15 mL) were added H₂O₂ (30% v/w, 2.05 mL, 16.2 mmol) and LiOH·H₂O (0.34 g, 8.1 mmol), and the solution was stirred at 0 °C for 1 h. The reaction was quenched with Na₂SO₃ (2.24 g in H₂O, 15 mL, 17.8 mmol). The pH was adjusted to ~4 with 10% aqueous citric acid and the mixture diluted with EtOAc. The aqueous fraction was extracted once more with EtOAc (50 mL), and the combined EtOAc layer was washed twice with brine (50 mL), dried over anhydrous MgSO₄, and evaporated to dryness under vacuum. The residue obtained was purified by flash column chromatography (using 20% hexane in EtOAc as the eluent) to give the free carboxylic acid **20b** as a pale yellow oil (0.76 g, yield 70%): ¹H NMR (400 MHz, DMSO-*d*₆) δ 1.21–1.35 (m, 6H), 1.38 (s, 9H), 1.50–1.65 (m, 2H), 2.00 (q, *J* = 6.9 Hz, 2H), 3.83 (m, 1H), 4.93 (dm, *J* = 10.2 Hz, 1H), 5.00 (dm, *J* = 17.0 Hz, 1H), 5.79 (tdd, *J* = 6.7, 17.0, 10.2 Hz, 1H), 7.01 (d, *J* = 8.0 Hz, 1H), 12.35 (br, 1H); ES⁺ MS *m/z* 272.4 (M + H)⁺.

Dipeptides 23a. To a solution of derivative **8** (1.19 g, 3.35 mmol, in 30 mL of THF) was added *t*-Bu₄NF (6.7 mL of 1 M in THF, 6.7 mmol), and the mixture was first stirred at rt for 16 h and subsequently heated to reflux for 15 min. The solvent was carefully evaporated under low pressure (due to the high volatility of the *tert*-butyl ester of **10**, caution should be exercised during the evaporation of the solvent). The crude residue was redissolved in EtOAc (100 mL), washed with H₂O (2 × 50 mL) and brine (50 mL), and dried over MgSO₄. After careful evaporation of the solvent under vacuum, an aliquot of this racemic compound (**10**)⁵³ was coupled with the P2 derivative **15a** following the standard protocol. The crude products was purified by flash column chromatography (using ~8–10% diethyl ether in EtOAc as the eluent) to obtain a pure sample of the set of diastereomers **23a** and **24a**. Each diastereomerically pure product was isolated in ~20% yield, however, the absolute stereochemistry was not assigned at this stage.

(53) The methyl-(1*R*,2*S*)/(1*S*,2*R*)-1-amino-2-homoallylcyclopropyl carboxylate (**10**) was also prepared by first treating compound **8** (1.74 g, 4.89 mmol) with a mixture of TFA/CH₂Cl₂ (20 mL, 1:1 ratio), and then with CH₂N₂. The unreacted CH₂N₂ was quenched with a few drops of acetic acid, 4 N HCl in dioxane (1.5 mL) was added and the solvents were evaporated to dryness to give the crude HCl salt of compound **10**. Fairly pure compound **10** was obtained after trituration in diethyl ether/hexane (3 × 5 mL, 1:1 ratio). ¹H NMR (400 MHz, CDCl₃) δ 1.45–1.49 (m, 1H), 1.53–1.79 (m, 2H), 1.85–1.89 (m, 1H), 1.98–2.05 (m, 1H), 2.10–2.21 (m, 2H), 3.83 (s, 3H), 4.99 (d, *J* = 10.2 Hz, 1H), 5.07 (dd, *J* = 1.6, 17.2 Hz, 1H), 5.73–5.83 (m, 1H), 9.0 (bs, 2H).

Compounds 23a: ¹H NMR (CDCl₃) δ 1.14–1.35 (m, 1H), 1.44 (s, 9H), 1.45 (s, 9H), 1.62–1.78 (m, 4H), 2.09–2.22 (m, 2H), ~2.6 (bs, 1H), ~2.95 (bs, 1H), 3.77 (bs, 1H), 3.88 (bs, 1H), 4.44–4.55 (m, 1H), 4.98 (d, *J* = 10.2 Hz, 1H), 5.03 (dd, *J* = 1.6, 17.2 Hz, 1H), 5.24 (bs, 1H), 5.75–5.88 (m, 1H), 7.42–7.58 (m, 2H), 7.63–7.73 (m, 2H), 8.04 (d, *J* = 8.3 Hz, 1H), 8.11 (d, *J* = 8.3 Hz, 1H), 8.74 (d, *J* = 5.1 Hz, 1H); ES⁺ MS *m/z* 552.3 (M + H)⁺; ES[−] MS *m/z* 550.2 (M − H)[−].

Compounds 24a:⁵⁴ ¹H NMR (CDCl₃) δ 1.18–1.35 (m, 1H), 1.45 (bs, 18H), 1.50–1.60 (m, 1H), 1.60–1.78 (m, 3H), 2.11–2.22 (m, 2H), ~2.3 (bs, 1H), 2.93 (m, 1H), 3.75 (bs, 1H), 3.90 (bs, 1H), 4.45–4.58 (bs, 1H), 4.98 (d, *J* = 10.2 Hz, 1H), 5.07 (dd, *J* = 1.6, 17.2 Hz, 1H), 5.22 (bs, 1H), 5.78–5.88 (m, 1H), 7.45–7.58 (m, 2H), 7.65–7.75 (m, 2H), 8.05 (d, *J* = 8.3 Hz, 1H), 8.11 (d, *J* = 8.3 Hz, 1H), 8.74 (d, *J* = 5.1 Hz, 1H); ES⁺ MS *m/z* 552.3 (M + H)⁺; ES[−] MS *m/z* 550.2 (M − H)[−].

N-Boc-Protected Dipeptide Methyl Ester 25a. To a solution of *N*-Boc-protected, *tert*-butyl ester of dipeptides **23a** (68 mg, 0.123 mmol) in dry CH₂Cl₂ was added a solution of HCl in dioxane (4 M, 4 mL), and the mixture was stirred at rt for 1.5 h. The solvent was then evaporated and the residue dried under high vacuum. The residue was dissolved in dioxane/H₂O (5 mL, 4:1 ratio), Boc₂O (81 mg, 0.37 mmol) and NaHCO₃ (73 mg, 0.86 mmol) were added, and the reaction mixture was stirred at rt for 12 h. The mixture was diluted with H₂O (10 mL) and extracted with EtOAc (50 mL). The aqueous layer was acidified to pH 4 and re-extracted with CH₂Cl₂ (2 × 100 mL). The combined CH₂Cl₂ layers were dried over anhydrous MgSO₄ and evaporated to dryness under reduced pressure. The residue was purified by flash column chromatography, using 3% EtOH in EtOAc as the eluting solvent, to obtain the pure P2 *N*-Boc protected, P1 free acid dipeptide intermediate. This intermediate was dissolved in diethyl ether/MeOH (3:2 mL, respectively) and treated with a slight excess of diazomethane dissolved in diethyl ether. After 30 min, the excess diazomethane was destroyed with the addition of HCl (a drop of 4 M in dioxane), and the mixture was evaporated to dryness to obtain the *N*-Boc-protected methyl ester **25a**: ¹H NMR (CDCl₃) mixture of rotamers (~1:9 ratio) δ (major rotamer) 1.22–1.35 (m, 2H), 1.42 (s, 9H), 1.55–1.62 (m, 1H), 1.62–1.74 (m, 2H), 2.06–2.18 (m, 2H), 2.32 (bs, 1H), 2.94 (bs, 1H), 3.71 (s, 3H), 3.70–3.90 (m, 2H), 4.55 (bs, 1H), 4.96 (dd, *J* = 0.95, 9.2 Hz, 1H), 5.03 (dm, *J* = 17.2 Hz, 1H), 5.27 (bs, 1H), 5.75–5.83 (m, 1H), 6.77 (bs, 1H), 7.49 (ddd, *J* = 1.3, 1.3, 8.3 Hz, 1H), 7.61 (bs, 1H), 7.70 (ddd, *J* = 1.3, 1.3, 8.3 Hz, 1H), 8.04 (d, *J* = 8.6 Hz, 1H), 8.15 (d, *J* = 8.0 Hz, 1H), 8.75 (d, *J* = 5.1 Hz, 1H); ES⁺ MS *m/z* 510.3 (M + H)⁺; ES[−] MS *m/z* 508.2 (M − H)[−].

Acyclic Diene 30a. The dipeptides **25a** was first treated with HCl (4 N in dioxane, ~20 equiv) over a period of 1.5 h at rt. The reaction mixture was concentrated under reduced pressure, and the resulting free amine (HCl salt form) was coupled with the P3 linker **20a** under the standard reaction conditions for amide bond formation. The crude product was purified by flash column chromatography (using 2% EtOH in EtOAc) to afford the corresponding diene **30a** as a white foam (~70% yield): ¹H NMR (CDCl₃, rotamers in ~10:1 ratio) δ (major rotamer) 1.21–1.27 (m, 1H), 1.36 (s, 9H), 1.45–1.81 (m, 8H), 2.02–2.20 (m, 4H), 2.25–2.35 (m, 1H), 2.92–3.02 (m, 1H), 3.66 (s, 3H), 3.94–3.98 (dd, *J* = 5.1, 11 Hz, 1H), 4.29–4.30 (bd, *J* = 9.9 Hz, 1H), 4.44–4.52 (m, 1H), 4.82 (dd, *J* = 5.4, 8.3 Hz, 1H), 4.92–5.06 (m, 4H), 5.14 (d, *J* = 8.3 Hz, 1H), 5.34–5.40 (m, 1H), 5.70–5.84 (m, 2H), 6.82 (d, *J* = 5.1 Hz, 1H), 7.47–7.55 (m, 2H), 7.71 (dt, *J* = 1.3, 7.5 Hz, 1H), 8.03 (d, *J* = 8.2 Hz, 1H), 8.17 (d, *J* = 8.0 Hz, 1H), 8.78 (d, *J* = 5.1 Hz, 1H); ES⁺ MS *m/z* 635.5 (M + H)⁺; ES[−] MS *m/z* 633.2 (M − H)[−].

Acyclic Ligand 30b. A sample of the tripeptide diene **30a** was saponified and purified by semipreparative C₁₈ reversed-

(54) Compound **24a** was converted to the macrocyclic inhibitor **26** using the same procedure as for the preparation of its epimer compound **33b**. In the enzymatic *in vitro* assay, compound **26** was found to be 40-fold less potent than **33b**.

phase HPLC (using the standard protocols) to give the free acid ligand **30b** as an amorphous white solid in >98.5% homogeneity, as determined by analytical HPLC method A: $t_R = 19.2$ min; ^1H NMR (DMSO- d_6 , rotamers in ~3.5:1 ratio) δ (major rotamer) 1.23 (s, 9H), 1.2–1.5 (m, 6H), 1.52–1.64 (m, 3H), 1.92–2.02 (m, 2H), 2.02–2.18 (m, 2H), 2.26–2.33 (m, 1H), 2.52–2.62 (m, 1H), 3.98 (bd, $J = 9.2$ Hz, 1H), 4.10 (bd, $J = 7.0$ Hz, 1H), 4.34–4.49 (m, 2H), 4.93 (bd, $J = 8.9$ Hz, 2H), 5.00 (d, $J = 17.2$ Hz, 2H), 5.64 (bs, 1H), 5.73–5.89 (m, 2H), 7.12 (d, $J = 7.3$ Hz, 1H), 7.28 (s, 1H), 7.48 (bs, 1H), 7.71 (dd, $J = 7.6$ Hz, 1H), 7.99 (dd, $J = 7.4$, 7.9 Hz, 1H), 8.09 (d, $J = 8.3$ Hz, 1H), 8.34 (d, $J = 8.0$ Hz, 1H), 9.08 (bd, $J = 5.1$ Hz, 1H); ES⁺ MS m/z 621.2 (M + H)⁺, 643.2 (M + Na)⁺; ES[−] MS m/z 619.1 (M − H)[−].

Macrocyclic Inhibitor 33b. Tripeptide diene **30a** was cyclized using the standard RCM reaction conditions. After completion of the reaction, the solvent was evaporated and the crude product was purified by flash column chromatography using 4% EtOH in EtOAc as the eluting solvent to give 50% yield of macrocyclic ester **33a** as a mixture of the *E* and *Z* double bonds. After saponification of the ester, under standard conditions, the mixture was purified by semipreparative C₁₈ reversed-phase HPLC, using a solvent gradient from 0 to 40% aqueous CH₃CN (0.06% TFA), to isolate the pure *E*-isomer, compound **33b**, as a white amorphous solid in >93% homogeneity, as determined by analytical HPLC method A: $t_R = 16.6$ min; ^1H NMR (DMSO- d_6) δ 1.12 (s, 9H), 1.20–1.24 (m, 2H), 1.32–1.40 (m, 3H), 1.58–1.62 (m, 2H), 1.68–1.78 (m, 3H), 1.95–2.02 (m, 1H), 2.08–2.18 (m, 2H), 2.42–2.59 (m, 2H), 3.97–3.40 (bd, $J = 9.8$ Hz, 2H), 4.47 (t, $J = 8.6$ Hz, 1H), 4.58 (d, $J = 11.8$ Hz, 1H), 5.22–5.29 (m, 1H), 5.46–5.54 (m, 1H), 5.66 (s, 1H), 7.12 (d, $J = 6.0$ Hz, 1H), 7.49 (d, $J = 3.5$ Hz, 1H), 7.68 (t, $J = 7.3$ Hz, 1H), 7.98 (t, $J = 7.0$ Hz, 1H), 8.08 (d, $J = 8.3$ Hz, 1H), 8.21 (s, 1H), 8.35 (d, $J = 8.3$ Hz, 1H), 9.08 (d, $J = 5$ Hz, 1H); FAB HRMS m/z found 593.297620 (M + H)⁺, calcd for C₃₂H₄₁N₄O₇ 593.297525.

Macrocyclic Inhibitor 33c. An sample of the methyl ester derivative of compound **33a** (20 mg, 0.033 mmol) in dry CH₂Cl₂ (1 mL) was stirred in the presence of 4 M HCl/dioxane (5 mL) for 1 h. The mixture was evaporated and dried carefully. The residue was redissolved in CH₂Cl₂/DMF (3 mL/1 mL), treated with NMM (14.5 μL , 0.132 mmol) and acetic anhydride (7.0 μL , 0.073 mmol), and stirred at rt for 14 h. The mixture was evaporated and dried under high vacuum. The residue was then dissolved in a mixture of THF/MeOH/H₂O (4 mL/2 mL/2 mL) and stirred overnight with LiOH·2H₂O (11 mg, 0.264 mmol). The residue isolated after acidification to pH = 3 with 1 N ice-cold HCl was purified by C₁₈ reversed-phase HPLC using a solvent gradient from 0 to 40% aqueous CH₃CN (0.06% TFA) in order to isolated pure compound **33c** as an amorphous white solid in >90% homogeneity, as determined by analytical HPLC method A: $t_R = 12.0$ min; ^1H NMR (50 mM Na₂PO₄ buffer, pH = 6.0, 600 MHz) δ 1.22–1.27 (m, 2H), 1.38–1.43 (m, 2H), 1.58–1.64 (m, 2H), 1.67–1.76 (m, 2H), 1.77–1.84 (m, 1H), 1.92–1.99 (m, 1H), 2.22–2.08 (m, 1H), 2.12–2.27 (m, 1H), 2.22–2.27 (m, 1H), 2.60–2.67 (m, 1H, Pro- β_-), 2.83–2.89 (m, 1H, Pro- β_+), 4.32 (dd, $J = 12.1$, 3.5 Hz, 1H, Pro- δ'), 4.41 (dd, $J = 12.1$, 7.3 Hz, 1H), 4.56 (bd, $J = 8.0$ Hz, 1H, Pro- δ), 4.62 (dd, $J = 8.9$ Hz, 1H, Pro- α), 5.40–5.46 (m, 1H), 5.55–5.61 (m, 1H), 5.73 (bs, 1H, Pro- γ), 7.41 (d, $J = 6.3$ Hz, 1H), 7.64 (bs, 1H, Acca-NH), 7.80 (dd, $J = 7.9$ Hz, 1H), 8.03 (dd, $J = 8.0$ Hz, 1H), 8.07 (d, $J = 9.5$ Hz, 1H), 8.16 (d, $J = 7$ Hz, 1H, AcNH), 8.36 (d, $J = 8.3$ Hz, 1H), 8.90 (d, $J = 6.0$ Hz, 1H); ES⁺ MS m/z 535.5 (M + H)⁺; ES[−] MS m/z 533.5 (M − H)[−].

Macrocyclic inhibitor 34a: white amorphous solid in >97% homogeneity, as determined by analytical HPLC method A: $t_R = 19.7$ min; ^1H NMR (DMSO- d_6) δ 1.17 (s, 9H), 1.16–1.25 (m, 2H), 1.28–1.37 (m, 3H), 1.52–1.65 (m, 2H), 1.65–1.83 (m, 3H), 1.92–2.05 (m, 1H), 2.05–2.20 (m, 2H), 2.39–2.48 (m, 1H), 2.58–2.68 (m, 1H), 3.94 (br, 2H), 3.97 (s, 3H), 4.45–4.49 (dd, $J = 7.6$, 9.5 Hz, 1H), 4.62 (brd, $J = 12.4$ Hz, 1H), 5.22–5.29 (m, 1H, *He*), 5.47–5.54 (m, 1H, *H η*), 5.82 (br,

1H), 7.10 (d, $J = 5.7$ Hz, 1H), 7.25 (brd, $J = 8.0$ Hz, 1H), 7.56 (br, 1H), 7.71 (br, 4H), 8.16–8.21 (br, 3H), 8.28 (d, $J = 13.3$ Hz, 1H). ^1H NMR decoupling experiments, via selective irradiation of the methylene protons adjacent to the olefinic protons [5.22–5.29 (m, 1H, *He*), 5.47–5.54 (m, 1H, *H η*)], resulted in $J = 15.2$ Hz between *He* and *H η* , confirming a trans geometry of the double bond (the details of the NMR spectra are available in the Supporting Information): ES⁺ MS m/z 699.3 (M + H)⁺; ES[−] MS m/z 697.3 (M − H)[−].

Macrocyclic inhibitor 34b: white amorphous solid in >92% homogeneity with respect to **34b** (sample contains ~17% of **34a**), as determined by analytical HPLC method A: $t_R = 20.1$ min; ^1H NMR (DMSO- d_6) δ ~1.0–1.2 (m, 3H), 1.24 (s, 9H), ~1.2–1.4 (m, 2H), ~1.4–1.6 (m, 1H), ~1.6–1.7 (m, 1H), ~1.7–1.8 (m, 3H), 1.99 (br, 1H), 2.20 (br, 1H), 2.25–2.35 (m, 1H), 2.40–2.50 (m, 1H), 2.50–2.68 (m, 1H), 3.96 (s, 3H), 4.05 (brd, $J = 9.2$ Hz, 1H), 4.22–4.28 (m, 1H), 4.44–4.49 (m, 2H), 5.22–5.30 (m, 1H, *He*), 5.42–5.50 (m, 1H, *H η*), 5.79 (br, 1H), 6.81 (br, 1H), 7.24 (d, $J = 7.6$ Hz, 1H), 7.52 (br, 1H), 7.62–7.70 (br, 4H), 8.05 (s, 1H), 8.15–8.26 (br, 3H). ^1H NMR decoupling experiments, via selective irradiation of the methylene protons adjacent to the olefinic protons [5.22–5.30 (m, 1H, *He*), 5.42–5.50 (m, 1H, *H η*)], resulted in $J = 10.4$ Hz between *He* and *H η* , confirming a cis geometry of the double bond (the details of the NMR spectra are available in the Supporting Information): ES⁺ MS m/z 699.4 (M + H)⁺; ES[−] MS m/z 697.3 (M − H)[−].

Macrocyclic inhibitor 35: white amorphous solid in >99% homogeneity, as determined by analytical HPLC method A: $t_R = 20.5$ min; ^1H NMR (DMSO- d_6) δ ~0.9–1.7 (m, 17H), 1.16 (s, 9H), 2.30–2.43 (m, 1H), 2.55–2.65 (m, 1H), 3.86 (bd, $J = 10.5$ Hz, 1H), 3.97 (s, 3H), 4.11 (br, 1H), 4.51–4.55 (dd, $J = 7.9$, 8.9 Hz, 1H), 4.66 (d, $J = 13.7$ Hz, 1H), 5.82 (br, 1H), 6.93 (d, $J = 5.7$ Hz, 1H), 7.27 (br, 1H), 7.55 (s, 1H), 7.69 (bs, 4H), 8.17 (bs, 2H), 8.21 (d, $J = 9.5$ Hz, 1H), 8.50 (s, 1H); ES⁺ HRMS m/z found 701.354636 (M + H)⁺, calcd for C₃₉H₄₉N₄O₈ 701.355040.

Macrocyclic inhibitor 36b: white amorphous solid in >99% homogeneity, as determined by analytical HPLC method A: $t_R = 20.0$ min; ^1H NMR (400 MHz, DMSO- d_6) δ 1.14 (s, 9H), 1.25–1.40 (bm, 7H), 1.45–1.51 (m, 2H), 1.65–1.75 (m, 2H), 2.13–2.19 (m, 1H), 2.33–2.42 (m, 1H), 2.56–2.70 (m, 2H), 3.87 (d, $J = 9.4$ Hz, 1H), 3.97 (s, 3H), 4.00 (br, 1H), 4.46–4.50 (dd, $J = 8.2$ Hz, 1H), 4.72 (d, $J = 11.2$ Hz, 1H), 5.24–5.29 (dd, $J = 9.5$ Hz, 1H), 5.49–5.56 (m, 1H), 5.82 (br, 1H), 7.12 (d, $J = 5.7$ Hz, 1H), 7.24 (br, 1H), 7.53 (s, 1H), 7.68 (br, 4H), 8.15–8.25 (m, 3H), 8.67 (s, 1H); ES⁺ HRMS m/z found 699.339469 (M + H)⁺, calcd for C₃₉H₄₇N₄O₈ 699.339390.

Acyclic Ligand 37. The P3 fragment **20a** was saturated under catalytic hydrogenation conditions. The Boc protecting group of dipeptide **27c** was removed under the usual acid conditions, and the saturated derivative of **20a** was coupled to this dipeptide to produce the tripeptide ester of **37**. After saponification of the ester (under the usual basic conditions) and purification of the acid products by C₁₈ reversed-phase HPLC, the pure ligand **37** was obtained as an amorphous white solid in >99% homogeneity, as determined by analytical HPLC method B: $t_R = 5.5$ min. ^1H NMR (DMSO- d_6 , mixture of rotamers in ~1:7 ratio) δ (major rotamer) 0.86 (t, $J = 6.8$ Hz, 3H), 1.05–1.12 (m, 1H), 1.22 (s, 9H), 1.15–1.55 (overlapping m, 9H), 2.02 (dd, $J = 8.6$, 17.1 Hz, 1H), 2.22–2.34 (m, 1H), 2.50–2.62 (m, 1H), 3.95 (s, 3H), 3.99 (bs, 1H), 4.13 (dd, $J = 8.3$, 14.3 Hz, 1H), 4.35–4.47 (m, 2H), 5.07 (dd, $J = 1.2$, 11.6 Hz, 1H), 5.20 (dd, $J = 1.2$, 17.3 Hz, 1H), 5.63–5.75 (m, 2H), 7.04 (d, $J = 7.2$ Hz, 1H), 7.18 (br, 1H), 7.46 (s, 1H), 7.50–7.68 (m, 4H), 8.13 (bs, 1H), 8.21 (bd, $J = 6.4$ Hz, 2H), 8.45 (s, 1H); ES⁺ HRMS m/z found (M + H)⁺ 701.354471, calcd for C₃₉H₄₉N₄O₈ 701.355040.

Macrocyclic Inhibitor 39b. The saturated macrocyclic methyl ester **39a** was saponified under basic conditions and purified by C₁₈ reversed-phase HPLC to obtain the macrocyclic inhibitor **39b** as a white solid in >99% homogeneity, as

determined by analytical HPLC method B: $t_R = 5.1$ min; ^1H NMR (DMSO- d_6) δ 1.11 (s, 9H), 1.15–1.45 (m, 13H), 1.60–1.90 (m, 3H), 2.35–2.41 (m, 1H), 2.64–2.68 (m, 1H), 3.96 (s, 3H), 4.05–4.11 (m, 1H), 4.14–4.20 (m, 1H), 4.31–4.35 (m, 2H), 4.50 (bd, $J = 10$ Hz, 1H), 5.80 (bs, 1H), 7.18 (d, $J = 8$ Hz, 1H), 7.26 (bd, $J = 9$ Hz, 1H), 7.54 (bs, 1H), 7.68 (bs, 4H), 7.81 (d, $J = 8$ Hz, 1H), 8.16 (d, $J = 4$ Hz, 2H), 8.23 (bd, $J = 8$ Hz, 1H); FAB HRMS m/z found 689.355070 ($M + H$) $^+$, calcd for $\text{C}_{38}\text{H}_{49}\text{N}_4\text{O}_8$ 689.355040.

Computational Chemistry Methods. A small fragment (**4**) representing the P1 portion of our inhibitors was utilized in quantum mechanics calculations to determine the rotational minima on each potential energy surface. Semiempirical calculations using Spartan 5.0 (Wave Function, Inc., Irvine, CA) were performed using PM3-SM3. The ϕ and ψ angles of **4** were rotated systematically while the remaining parameters were allowed to relax. Specifically, angles ϕ and ψ were varied by 15° to generate 144 points. Symmetry was exploited when possible. Each point was gradient minimized using the PM3-SM3 and the energy was plotted as a function of angles ϕ and ψ . Two energy minima (**4a** and **4b**) were identified from the above conformational energy profile. The global minimum corresponded to conformation **4a** and was characterized by a ϕ angle of $+98^\circ$. Another local minimum (**4b**), which was 1.1 kcal/mol higher in energy compared to **4a**, was also identified and was characterized by a ϕ angle of -98° .

NMR Sample Preparation. NMR samples were prepared by adding 24 μL of concentrated solution of inhibitor **33c** in DMSO- d_6 to an aqueous buffer composed of 50 mM Na_2PO_4 , 300 mM NaCl, 3 mM dithiothreitol- d_{10} , and 10% (v/v) D_2O (spiked with TSP) at pH 6.5. The final volume of these solutions was 600 μL with inhibitor concentrations ranging between 1 and 1.5 mM. Expression and purification of NS3 protease BK strain (spanning amino acids 1–180 and harbored the C-terminal poly Lys solubilization motif ASKKKK 8) which was used in the NMR experiments was previously described.¹⁷ For the transferred NOESY experiments, a concentrated stock solution of NS3 protease BK* poly Lys (9.2 mg/mL, ~ 450 μM , in a buffer identical to that previously described)¹⁷ was added to these samples such that an inhibitor/protease ratio of 20:1 to 25:1 was typically achieved. For the competition experiments, a stock solution of a potent hexapeptide **43** ($\text{IC}_{50} < 1$ nM)⁴⁹ in DMSO- d_6 (3.6 mM) was added to the samples described above such that a 3–4-fold excess of potent inhibitor vs protease was achieved.

NMR Methods. All spectra were acquired at 27°C . Two-dimensional (2D) double-quantum-filtered COSY (DQF-COSY), TOCSY, NOESY, and ROESY spectra were acquired using standard pulse sequences with time proportional phase incrementation (TPPI) method at 600 MHz. Suppression of the solvent signal was achieved by the use of presaturation or by inserting a 3–9–19 WATERGATE module prior to data acquisition. The 2D transferred-NOESY experiments were recorded with mixing time of 70, 100, 150, and 200 ms. In these experiments, a 25 ms spin-lock pulse was applied prior to t_1 delay in order to eliminate protein background signals.⁵⁵ The ROESY experiment was recorded with a 300 ms spin-lock period. The 2D data sets were typically acquired with 2048 points in t_2 , 350–512 points in t_1 , and 96–128 scans. The data were processed and analyzed using XWinNMR and WinNMR software (Bruker Canada, Milton, Ontario) and Felix software (Molecular Simulations, Inc., San Diego, CA). Shifted sinebell apodization and zero-filling (2048×1048 real points) were applied prior to Fourier transformation, and subsequent baseline corrections were applied in one or both dimensions.

Restrained Dynamics. The NS3-bound conformation of inhibitor **33c** was modeled by a simulating annealing protocol using Discover 98.0 and the CFF force field (Molecular Simulations, Inc., San Diego, CA). The dynamics were performed without cross-terms and nonbonded cutoffs and with

a dielectric constant of 80. A total of 43 NMR-derived distance restraints were generated from transferred-NOESY volume buildup rates using the Assign module of Felix software (Molecular Simulations, Inc., San Diego, CA). These NMR distance restraints were applied as strong (1.8–2.5 Å), medium (1.8–3.5 Å) or weak (1.8–5.0 Å) flat-bottomed potentials having force constants of 15 kcal/mol·Å 2 . Pseudoatoms defining the centroids of the methyl groups were introduced in the definition of the NOE restraints and the interproton distances were corrected accordingly.⁵⁶ A single, high-temperature unrestrained dynamics run was performed at 900 K using a time step of 1 fs, with 50 structures collected at 2 ps intervals to generate a starting set of conformations. Each structure was then retrieved, cooled, and minimized using the following simulated annealing protocol. The temperature was initially lowered to 750 K at a rate of 30 K/ps where only strong restraints were applied. The remaining restraints were added and additional cooling to first 500 K (25 K/ps) and then 300 K (20 K/ps) was performed, followed by restrained minimization (including cross-terms) to a final gradient of 0.005 kcal/mol·Å. A total of 10 low energy, NMR-consistent, structures were selected at the end of this protocol. These final 10 structures are shown superimposed (P1–P3 backbone atoms only) in Figure 3A. The root-mean-square deviation for the backbone atoms of P1–P3 is 0.04 Å. None of these structures have distance violations greater than 0.05 Å and the average total restraint violation energy is 0.03 kcal/mol with a S.D. = 0.01 kcal/mol.

Docking Protocol. The NS3 protease complex model of inhibitor **33c** was obtained from energy minimization and molecular dynamics using Discover 98.0 and the CFF force field (Molecular Simulations Inc., San Diego, CA). The dynamics were performed without cross-terms and nonbonded cutoffs and with a dielectric constant of 1. As a starting point for the simulation, the NS3 protease bound conformation of compound **33c** (as determined above) was docked into the substrate binding region of the X-ray crystal structure of the *apo* NS3 protease.^{50a} The inhibitor was appropriately oriented in order to allow its P1 carboxylate group to make H-bonds with the side chains of the catalytic triad residues H57 and S139, as well as with the backbone NH of the oxyanion hole residues S139 and G137 and in order to allow the formation of additional hydrogen bonds between the backbone NH and CO groups of the inhibitor P3 and the complementary backbone groups of the protein A157 residue. The bound inhibitor was then energy-minimized. The conformation of the protein, as well as the P1 carboxylate anion of the inhibitor, were kept fixed during this first minimization step. This initial complex model was subsequently soaked in a 20 Å sphere of water. The NS3 protein and the water molecules were then divided into three zones and tethered to different extent during the simulation. Zone 1: 0–10 Å away from the center of mass of the inhibitor, Zone 2: 10–15 Å away from the inhibitor, Zone 3: >15 Å away from the inhibitor. The entire complex was first submitted to energy-minimization and then to 1 ns of dynamics at 298 K following a 200 ps equilibration step. Zone 3 was kept fixed during this entire simulation, while zone 2 and zone 1 were tethered using quadratic force constants of 10 and 1 kcal/mol·Å 2 respectively during the initial minimization step. These tethering force constants were then gradually reduced during the dynamic equilibration steps, and were totally removed during the 1 ns dynamic run. In addition, the inhibitor P1 carboxylate was also tethered using a quadratic force constant of 1 kcal/mol·Å 2 during the initial steps. The bond lengths and water molecule angles were kept fixed during the entire dynamic simulation using rattle. At the end of the dynamics the complex was further minimized (including cross-terms) to a final gradient of 0.1 kcal/mol·Å.

(55) Scherf, T.; Anglister, J. A. *Biophys. J.* **1993**, *64*, 754.

(56) Wüthrich, K.; Billeter, M.; Braun, W.; Anglister, J. J. *Biol. Mol.* **1983**, *169*, 949.

Acknowledgment. We thank Ms. Diane Thibeault and Mr. Roger Maurice for the in vitro enzymatic assays and Dr. Steven LaPlante and Mr. Norman Aubry for assistance with some of the NMR data. We thank Dr. Lynn Amon for valuable discussions regarding some of the computational data. We thank Mr. Chris Bryan for assistance in the preparation of some intermediates and Ms. Vida Gorys for providing a sample of compound **3**. We also wish to thank Dr. Pierre Bonneau and Ms. Céline Plouffe for purification of the NS3 protease enzyme. We are also grateful to Dr. Jean Rancourt for his advice on the synthesis of compound **10**. We wish to thank Drs. Pierre Beaulieu and Jean Rancourt for assistance in proofreading the manuscript. Finally, we

thank Drs. Paul Anderson and Robert Déziel for their support of this project.

Supporting Information Available: Data of intermediates **5b**, **6b**, **15a,b**, **20a**, **21a,b**, **22a,b**, **23b**, **25b**, **27**, **28a,b**, **29a–d**, **30c**, **31**, **32b**, **39a**, **41a,b**, and **42**. ¹H NMR spectra and decoupling experiments of the final inhibitors used in the SAR studies (Scheme 2: **26**, **29c,d**, **30b**, **32b**, **33b,c**, **34a,b**, **35**, **36b**, **37**, **39b**, **41b**, and **42**); the chemical shift assignments (as indicated) were confirmed by multiple 2D NMR experiments. 2D TRNOESY data relevant to the determination of the NS3-bound conformation of ligand **33c**, as well as the competition study with hexapeptide **43** (Figure 1). This material is available free of charge via the Internet at <http://pubs.acs.org>.

JO049288R